Syndecan-1 regulates $\alpha_v\beta_3$ and $\alpha_v\beta_5$ integrin activation during angiogenesis and is blocked by synstatin, a novel peptide inhibitor

DeannaLee M. Beauvais, Brian J. Ell, Andrea R. McWhorter, and Alan C. Rapraeger

Department of Pathology and Laboratory Medicine, University of Wisconsin-Madison, Madison, WI 53706

Syndecan-1 (Sdc1) is a matrix receptor shown to associate via its extracellular domain with the $\alpha_v\beta_3$ and $\alpha_v\beta_5$ integrins, potentially regulating cell adhesion, spreading, and invasion of cells expressing these integrins. Using Sdc1 deletion mutants expressed in human mammary carcinoma cells, we identified the active site within the Sdc1 core protein and derived a peptide inhibitor called synstatin (SSTN) that disrupts Sdc1's interaction with these integrins. Because the $\alpha_v\beta_3$ and $\alpha_v\beta_5$ integrins are critical in angiogenesis, a process in which a role for Sdc1 has been uncertain, we used human vascular endothelial cells in vitro to show that the Sdc1 regulatory mechanism is also required for integrin activation on these cells. We found Sdc1 expressed in the vascular endothelium during microvessel outgrowth from aortic explants in vitro and in mouse mammary tumors in vivo. Moreover, we show that SSTN blocks angiogenesis in vitro or when delivered systemically in a mouse model of angiogenesis in vivo, and impairs mammary tumor growth in an orthotopic mouse tumor model. Thus, Sdc1 is a critical regulator of these two important integrins during angiogenesis and tumorigenesis, and is inhibited by the novel SSTN peptide.

CORRESPONDENCE
Alan C. Rapraeger:
acraprae@wisc.edu

Abbreviations used: FGF, fibroblast growth factor; FN, fibronectin; GST, glutathione S-transferase; HAEC, human aortic endothelial cell; HMEC-1, human dermal microvascular endothelial cell; HS, heparan sulfate; hSdc1, human Sdc1; HUVEC, human umbilical vein endothelial cell; MAEC, mouse aortic endothelial cell; mSdc1, mouse Sdc1; OCT, optimum cutting temperature; PECAM-1, platelet–endothelial cell adhesion molecule–1; Poly-HEMA, poly(2-hydroxyethyl methacrylate); siRNA, small interfering RNA; Sdc1, syndecan-1; S1ED, Sdc1 extracellular domain; SSTN, synstatin; VEGF, vascular endothelial growth factor; VN, vitronectin.

Angiogenesis, or the sprouting of new blood vessels from existing ones, occurs during development and in diseases such as diabetic retinopathy, endometriosis, psoriasis, rheumatoid arthritis, and tumor-induced angiogenesis (1). Vascular endothelial cells rely on signaling from multiple integrins during the angiogenic process (for review see reference 2), including the $\alpha_v\beta_3$ and $\alpha_v\beta_5$ integrins; signaling by the $\alpha_v\beta_3$ and $\alpha_v\beta_5$ integrin leads to endothelial cell proliferation, migration, matrix metalloprotease activation, and resistance to apoptosis (3).

The $\alpha_v\beta_3$ and $\alpha_v\beta_5$ integrins are subject to regulation during angiogenesis. Fibroblast growth factor (FGF) and vascular endothelial growth factor (VEGF), two potent angiogenic factors released by tumors, induce the expression of these two integrins that collaborate with the FGF and VEGF receptors in angiogenic signaling pathways (4); disrupting angiogenic signaling by inactivation of either integrin or growth factor receptor leads to endothelial cell apoptosis (5). The integrins are often up-regulated on metastatic tumors as well, leading to enhanced invasion, proliferation, and tumor survival (6–9) by largely the same mechanisms operative in endothelial cells. For these reasons, the integrins and their regulatory mechanisms are attractive targets for the development of therapeutic drugs. Drugs that are currently being tested range from inhibitory integrin antibodies (e.g., Vitaxin [10], based on the inhibitory antibody LM609 [11]), to cyclic RGD peptides that interfere with ligand binding (e.g., cRGDfV, cilengitide, and ST1646 [12–15]), to peptidomimetics based on the RGD sequence (e.g., S247 [16]). These inhibitors have all been shown to disrupt the growth of solid tumors as well as angiogenesis.

We have recently identified a regulatory mechanism by which syndecan-1 (Sdc1), a cell-surface matrix receptor, regulates the activation of the $\alpha_v\beta_3$ and $\alpha_v\beta_5$ integrins on mammary carcinoma cells and fibroblasts (17–20). The syndecans are multifunctional extracellular matrix

D.M. Beauvais and B.J. Ell contributed equally to this paper.

The Rockefeller University Press $30.00
J. Exp. Med. Vol. 206 No. 3 691-705
www.jem.org/cgi/doi/10.1084/jem.20081278

receptors on the surface of all adherent cells (21–23). They anchor to the matrix via heparan sulfate (HS) glycosaminoglycan chains attached near the distal tips of their core proteins; these chains recognize "heparin-binding" domains present in most matrix ligands, including fibronectin (FN), laminins, vitronectin (VN), thrombospondin, and the fibrillar collagens (21). In addition, mounting evidence suggests that they assemble with and control the signaling of other cell surface receptors, including integrins. McFall et al. first described a "cell-binding domain" in the extracellular domain of Sdc4 (24, 25); this site has recently been shown to regulate β1-containing integrins on mesenchymal cells, although the exact integrin target and regulatory mechanism remain unknown (26, 27). Recombinant Sdc2 extracellular domain alters adhesion mechanisms in colon carcinoma cells, suggesting that a regulatory site also exists in its extracellular domain (28, 29). More recently, we have shown that Sdc1 is necessary for activation of the $\alpha_v\beta_3$ integrin on mammary carcinoma cells (17, 20). Silencing Sdc1 expression, selective deletion of amino acids in its extracellular domain, or targeted competition with domain-specific antibodies or recombinant extracellular domain protein disrupts integrin activation and matrix recognition necessary for cell spreading and invasion. Similar activation of the $\alpha_v\beta_5$ integrin by Sdc1 occurs on B82L fibroblasts, which rely exclusively on this integrin for attachment to VN and FN (19). These extracellular syndecan-specific regulatory sites are readily accessible to therapeutic drugs and may hold promise as targets for combating tumorigenesis and other diseases in which their regulated mechanisms play a role.

Given the importance of the $\alpha_v\beta_3$ and $\alpha_v\beta_5$ integrins in angiogenesis, we examined the possibility that Sdc1 regulates these integrins on vascular endothelial cells during tumor-induced angiogenesis. We found that Sdc1 is expressed by mouse and human endothelial cells in vitro, and is expressed during angiogenesis induced by FGF or VEGF in vitro and in vivo. We found that the $\alpha_v\beta_3$ and $\alpha_v\beta_5$ integrins associate with Sdc1 and that this association can be disrupted by a peptide called synstatin (SSTN) that is derived from the active site in the Sdc1 core protein. Furthermore, SSTN is an effective inhibitor of angiogenesis in vitro and in vivo, and of mammary carcinoma formation in nude mice. These results define the Sdc1 regulatory mechanism as a critical component of the angiogenic and tumorigenic process.

RESULTS

SSTN peptide inhibits Sdc1-mediated activation of the $\alpha_v\beta_3$ integrin on mammary carcinoma cells

MDA-MB-231 human mammary carcinoma cells rely on Sdc1 for activation of the $\alpha_v\beta_3$ integrin during their binding and spreading on VN (17, 20). Integrin activity is abolished by silencing Sdc1 expression with human-specific small interfering RNA (siRNA) but can be rescued by expression of mouse Sdc1 (mSdc1; Fig. 1 B). Cell binding and spreading on FN, which utilizes the $\alpha_5\beta_1$ integrin, is unaffected (Fig. 1 B) (20). Although native mSdc1 rescues integrin activity, deletion mutants (summarized in Fig. 1 A) (20) lacking a putative active site between amino acids 88 and 121 in its extracellular domain fail to rescue (see mSdc1Δ67–121; Fig. 1 B).

We showed previously (20) that $\alpha_v\beta_3$ integrin activity is lost in MDA-MB-231 cell adhesion/spreading assays in the presence of soluble, recombinant glutathione S-transferase–fused Sdc1 extracellular domain (GST-S1ED; ID_{50} of ~3 μM). To test whether shorter peptides would mimic this activity, we derived a peptide spanning amino acids 82–130 of mSdc1 (Fig. 1 A). We call the inhibitory peptide sequence SSTN. Indeed, treatment of MDA-MB-231 cells with $SSTN_{82\text{-}130}$ blocks their spreading on VN but not FN (Fig. 1 C).

We hypothesize that S1ED or $SSTN_{82\text{-}130}$ may compete for an interaction between the S1ED and the $\alpha_v\beta_3$ integrin. To assess this, immunoprecipitations were performed using MDA-MB-231 cells expressing either empty vector (NEO), ectopic full-length mSdc1, or the mSdc1Δ67–121 deletion mutant that lacks the active site. Immunoblotting reveals that the $\alpha_v\beta_3$ integrin coprecipitates with either native human Sdc1 (hSdc1) or ectopic mSdc1, yet fails to associate with the mSdc1 mutant bearing the Δ67–121 deletion (Fig. 1 D). Coprecipitation is disrupted in the presence of either 30 μM GST-S1ED protein (using either mS1ED or hS1ED to avoid reactivity with the precipitating mAb) or 3 μM $SSTN_{82\text{-}130}$ (which is not recognized by either precipitating mAb). These results suggest that these inhibitors block $\alpha_v\beta_3$ integrin activation by competitively displacing the integrin from an interaction with Sdc1.

To define the minimal sequence required, we tested SSTN peptides (0–100 μM) carrying sequential N- and C-terminal deletions (Fig. 2 C) for their ability to block cell spreading on VN (Fig. 2, A and B). The minimal peptide required for full activity is $SSTN_{92\text{-}119}$. Deletion of two or three residues from either end of this peptide either diminishes (approximately threefold loss in activity in $SSTN_{88\text{-}117}$) or completely abolishes ($SSTN_{94\text{-}119}$ and $SSTN_{88\text{-}116}$) activity. A peptide representing the homologous region of hSdc1, $hSSTN_{89\text{-}120}$, is equally effective as an inhibitor (Fig. 2 C), confirming that the active site is conserved between hSdc1 and mSdc1. Peptides displayed identical inhibitory effects on B82L fibroblasts, which rely solely on the $\alpha_v\beta_5$ integrin for adhesion and spreading on VN (unpublished data) (19).

Sdc1 regulates the $\alpha_v\beta_3$ and $\alpha_v\beta_5$ integrins on vascular endothelial cells

We next questioned whether the Sdc1 regulatory mechanism is operative on vascular endothelial cells. Human aortic endothelial cells (HAECs) and human dermal microvascular endothelial cells (HMEC-1s) express modest levels of Sdc1 and higher levels of $\alpha_v\beta_3$ and $\alpha_v\beta_5$ integrins (Fig. 3 A). Mouse aortic endothelial cells (MAECs) express higher levels of Sdc1 than their human counterparts but less of the two integrins (Fig. 3 A).

To determine if Sdc1 and the integrins are in a regulatory complex, immunoprecipitates from HMEC-1s were probed for the coprecipitation of β_3 and β_5 integrin subunits with Sdc1. Both integrins coprecipitate with the syndecan and

in seemingly equal proportions (quantified via comparison to a whole-cell lysate standard curve; not depicted) suggestive of a 1:1 correspondence (Fig. 3 B). The $\alpha_v\beta_1$ integrin, which is not regulated by Sdc1 (17, 19, 20), fails to coprecipitate (unpublished data). Immunoprecipitations were also conducted in the presence of either 30 μM GST-mS1ED or 3 μM $SSTN_{82-130}$, $SSTN_{92-119}$, or $SSTN_{94-119}$; note that none of these are recognized by the human-specific mAb used for precipitation (Fig. 3 B). As expected, both the GST-mS1ED protein (but not GST alone) and the

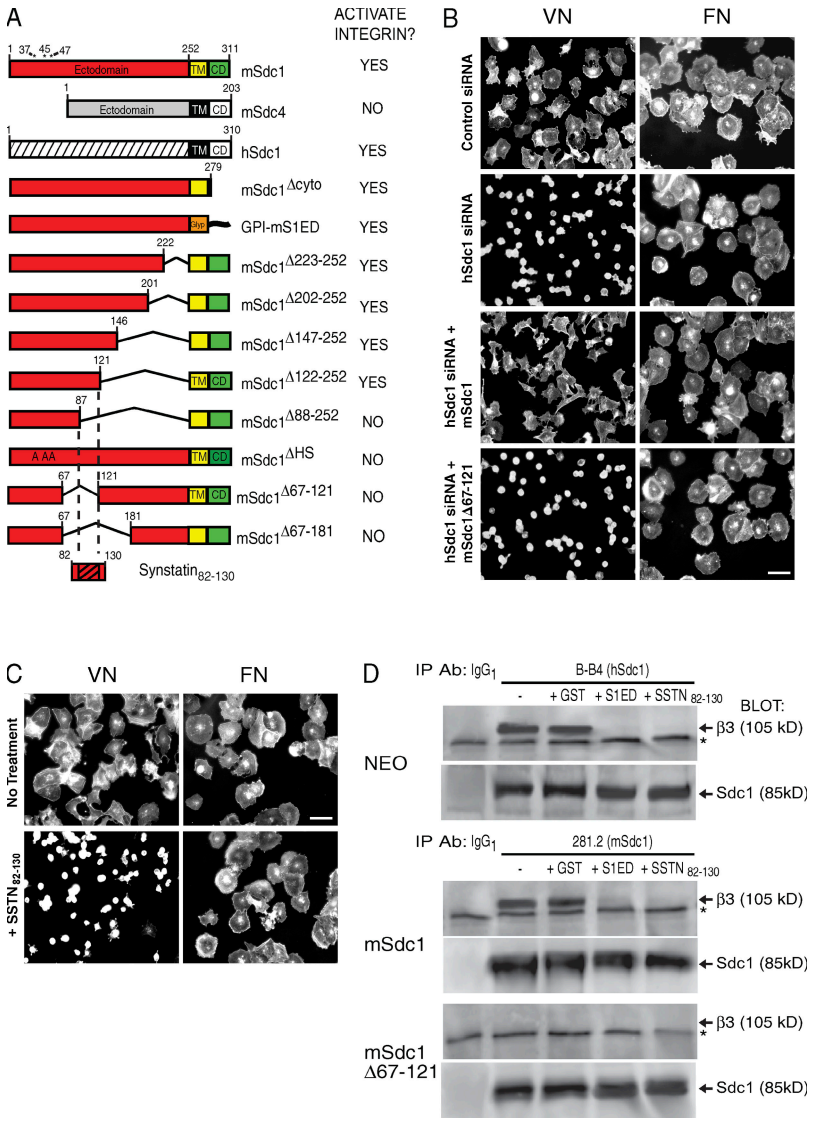

Figure 1. Derivation of SSTN peptide. (A) Summary of $\alpha_v\beta_3$ or $\alpha_v\beta_5$ integrin activation in cell attachment/spreading assays by either native or mutant mSdc1, mSdc4, or hSdc1 (reference 20). Numbers refer to mouse amino acid sequence. HS attachment sites in Sdc1 are amino acids 37, 45, and 47. Deletions identify a putative active site between amino acids 88–121; this site is contained in an SSTN peptide encompassing amino acids 82–130 ($SSTN_{82-130}$). CD, cytoplasmic domain; GPI, glycosylphosphatidylinositol-linked lipid tail; TM, transmembrane domain. (B) $mSdc1^{\Delta 67-121}$ deletion mutant fails to activate the $\alpha_v\beta_3$ integrin. Spreading of MDA-MB-231 cells for 2 h on either VN ($\alpha_v\beta_3$ dependent) or FN ($\alpha_v\beta_3$ independent) after silencing of hSdc1 expression with human-specific siRNA and rescue with either mSdc1 or $mSdc1^{\Delta 67-121}$ deletion mutant. All images represent results from triplicate wells and three independent experiments. Bar, 50 μm. (C) Spreading of MDA-MB-231 cells on VN or FN in the presence or absence of 1 μM $SSTN_{82-130}$. Bar, 50 μm. (D) SSTN disrupts Sdc1 coimmunoprecipitation with the $\alpha_v\beta_3$ integrin. hSdc1 is immunoprecipitated (using mAb B-B4) from MDA-MB-231 cells transfected with empty vector (NEO), and mSdc1 is immunoprecipitated (using mAb 281.2) from cells transfected with full-length mSdc1 or the mSdc1 deletion mutant ($mSdc1^{\Delta 67-121}$). Immunoprecipitations were conducted in the presence or absence of GST, GST-S1ED (mS1ED if precipitating hSdc1 and hS1ED for mSdc1 precipitation), or $SSTN_{82-130}$. Blots were probed for coprecipitation of β_3 integrin subunit (~105 kD) using Fire & Ice. Note the nonspecific band (*) that appears in all lanes, including the nonspecific IgG_1 isotype control precipitations. Sdc1 runs as a band at approximately 85 kD after treatment with enzymes to remove its glycosaminoglycan chains; the core protein is visualized on the blots using mAb 3G10, which detects HS attachment stubs remaining on either the hSdc1 or mSdc1 core protein. Results are representative of at least three independent experiments.

active $SSTN_{82-130}$ and $SSTN_{92-119}$ efficiently disrupt the Sdc1–integrin interactions, whereas the inactive $SSTN_{94-119}$ is without effect.

To test whether Sdc1 interacts directly with the integrins (Fig. 3 C), GST-mS1ED immobilized on glutathione beads was mixed in solution with 1 μM purified $\alpha_v\beta_3$ or $\alpha_v\beta_5$ integrin in the presence of 10 μM competitive $SSTN_{92-119}$ or noncompetitive $SSTN_{94-119}$. The purified integrins associate with S1ED, and their binding is competed by $SSTN_{92-119}$ but not by $SSTN_{94-119}$. In addition, $SSTN_{92-119}$ prelabeled with photoactivatable Sulfo-SBED cross-linker (see Materials and methods) binds and transfers biotin label to both the α and β subunits of purified $\alpha_v\beta_3$ integrin, whereas no transfer is detected with $SSTN_{94-119}$ (Fig. 3 D).

We next questioned whether the Sdc1 regulatory mechanism affects integrin activity on endothelial cells. Sdc1 expression was silenced in HMEC-1s using siRNA (Fig. 3 E, left), and the cells were plated on VN. Control siRNA–transfected cells bind and spread, but the spreading is blocked by >95% if Sdc1 expression is silenced (Fig. 3 E, right). Quantification of HMEC-1 and HAEC cell spreading (Fig. 3 F, left) or attachment (Fig. 3 F, right) shows that cell spreading is completely blocked, and cell attachment is blocked by 80% for both cell types when Sdc1 expression is reduced by ∼90% (Fig. 3 F). This is compared with combined treatment with 30 μg/ml $\alpha_v\beta_3$ and $\alpha_v\beta_5$ function–blocking antibodies LM609 and P1F6 (Fig. 3 F).

We next tested whether the SSTN peptides inhibit integrin activation on the endothelial cells. HMEC-1s were plated on hSdc1 antibody (mAb B-B4), to which the cells attach and spread (Fig. 4 A). Our previous work using carcinoma cells showed that Sdc1 ligation by this method leads to integrin activation and cell spreading (17), even in the presence of EDTA to block potential ligand binding by the integrin. Indeed, the $\alpha_v\beta_3$ and $\alpha_v\beta_5$ integrins become activated when the cells attach to B-B4, detected by staining the cells with the ligand-mimetic Fab WOW-1 (Fig. 4 A) (30). However, treatment with either 0.5 μM $SSTN_{82-130}$ or 30 μg/ml $\alpha_v\beta_3$ and $\alpha_v\beta_5$ integrin function–blocking antibodies (used as a comparative control) prevents both cell spreading and recognition by WOW-1, indicating that $SSTN_{82-130}$ inhibits integrin activation. A similar experiment was conducted using suspended human umbilical vein endothelial cells (HUVECs) in which cell-surface Sdc1 is first decorated with hSdc1-specific mAb B-A38 and then clustered by addition of a secondary antibody in the presence or

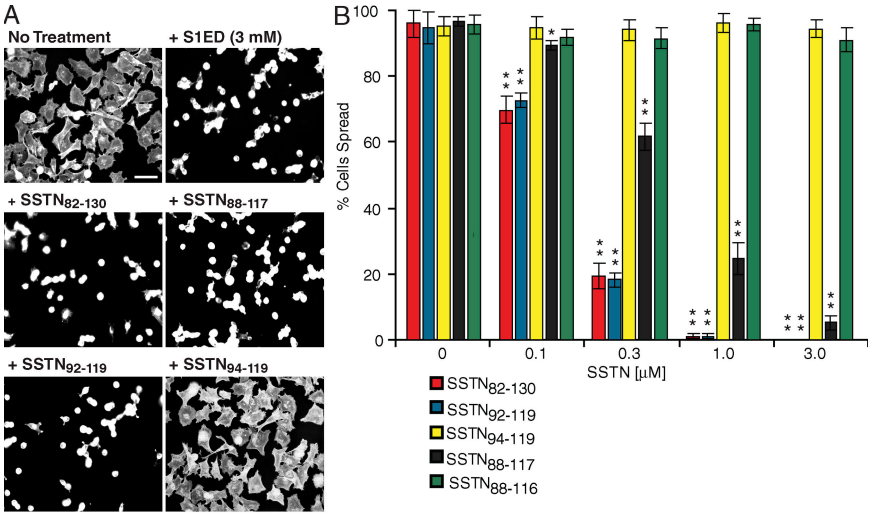

C

		ID_{50}
$SSTN_{82-130}$	^{82}SNTETAFTSVLPAGEKPEEGEPVLHVEAEPGFTARDKEKEVTTRPRETV^{130}	0.1-0.3
SSTN88-122	^{88}FTSVLPAGEKPEEGEPVLHVEAEPGFTARDKEKEV^{122}	0.1-0.3
SSTN88-117	^{88}FTSVLPAGEKPEEGEPVLHVEAEPGFTARD^{117}	0.3-1.0
SSTN88-116	^{88}FTSVLPAGEKPEEGEPVLHVEAEPGFTAR^{116}	>100
SSTN92-119	^{92}LPAGEKPEEGEPVLHVEAEPGFTARDKE^{119}	0.1-0.3
SSTN94-119	^{94}AGEKPEEGEPVLHVEAEPGFTARDKE^{119}	>100
Human SSTN	^{89}STSTLPAGEGPKEGEAVVLPEVEPGLTAREQE^{120}	0.1-0.3

Figure 2. Identification of minimal SSTN peptide. (A) Inhibition of MDA-MB-231 cell spreading on VN by SSTN. MDA-MB-231 cells were plated for 2 h on VN in the presence or absence of 3 μM mS1ED or 0.3 μM $SSTN_{82-130}$, $SSTN_{88-117}$, $SSTN_{92-119}$, or $SSTN_{94-119}$. Bar, 50 μm. (B) Quantification of cell spreading over a range of SSTN concentrations. Error bars represent SEM of triplicate points in each of two independent experiments. *, $P < 0.05$; **, $P < 0.01$). (C) Summary of SSTN peptides tested and their efficacy as inhibitors in the $\alpha_v\beta_3$-dependent MDA-MB-231 cell spreading assay. The active 92–119 sequence is underlined in the larger $SSTN_{82-130}$ sequence.

absence of $SSTN_{82-130}$. WOW-1 binding shows that clustering of Sdc1 activates the integrin, and this is prevented by the SSTN peptide (Fig. 4 B).

Blockade of integrin activation with the SSTN peptides is also shown by disrupted cell attachment and spreading on VN. HMEC-1s are dependent on both integrins, as partial

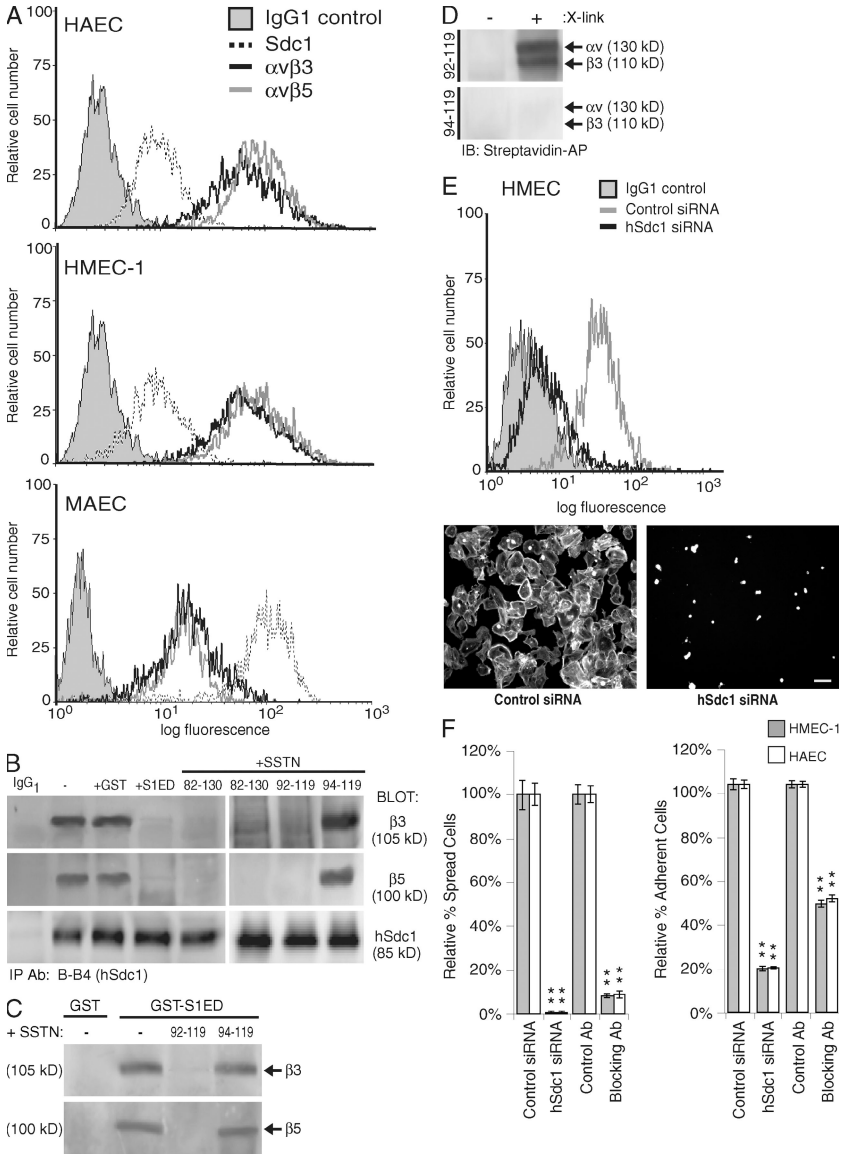

Figure 3. Expression of Sdc1 and $\alpha_v\beta_3$ and $\alpha_v\beta_5$ integrins in vascular endothelial cells. (A) Sdc1, $\alpha_v\beta_3$, or $\alpha_v\beta_5$ expression on HAECs, HMEC-1s, or MAECs is analyzed by flow cytometry. (B) SSTN competition for Sdc1 association with $\alpha_v\beta_3$ and $\alpha_v\beta_5$ integrins. hSdc1 is immunoprecipitated from HMEC-1s using mAb B-B4 in the absence or presence of 30 µM GST, 30 µM GST-S1ED, or 3 µM $SSTN_{82-130}$, $SSTN_{92-119}$, or $SSTN_{94-119}$. Blots are probed for Sdc1 precipitation (~85 kD) and for coprecipitating β_3 integrin (~105 kD) subunit using Fire & Ice, and β_5 subunit with AB1926 (~100 kD). (C) Sdc1 associates directly with purified $\alpha_v\beta_3$ or $\alpha_v\beta_5$ integrin and is competed by $SSTN_{92-119}$. Glutathione beads bearing GST-mS1ED were incubated with purified integrin in the presence or absence of $SSTN_{92-119}$ and $SSTN_{94-119}$. Integrin captured by the beads (or beads bearing GST alone) was detected on blots. Results are representative of at least three independent experiments. (D) Cross-linking $SSTN_{92-119}$ to $\alpha_v\beta_3$ integrin. $SSTN_{92-119}$ or $SSTN_{94-119}$ prelabeled with Sulfo-SBED, a UV photoactivatable biotin transfer reagent, was incubated with purified $\alpha_v\beta_3$ integrin, and the transfer of the biotin label from SSTN to the α_v and β_3 subunits was assessed by Western blot either with (X-link +) or without (X-link −) photoactivation of the cross-linker. Results are representative of duplicate samples and at least two independent experiments. (E) Dependence of $\alpha_v\beta_3$ and $\alpha_v\beta_5$ integrin activation on Sdc1 in HMEC-1s. (left) Sdc1 expression in HMEC-1s was detected by mAb B-B4 in flow cytometry with or without silencing expression with Sdc1-specific siRNA. (right) HMEC-1s were plated on VN for 2 h with or without silencing hSdc1 expression. Bar, 50 µm. (F) Effect of Sdc1 silencing on endothelial cell attachment and spreading. Quantification of the percentage of spread HMEC-1s and HAECs (left) or attached cells (right) after treatment with control or hSdc1-specific siRNA to silence Sdc1 expression, or compared with treating with 30 µg/ml $\alpha_v\beta_3$ integrin and $\alpha_v\beta_5$ integrin blocking antibodies LM609 and P1F6, respectively, versus an isotype control antibody to block integrin activity. Note that these antibody concentrations allow half-maximal binding. Results are representative of triplicate wells and at least two independent experiments. Data are presented as means ± SEM. **, $P < 0.01$.

spreading is observed if one integrin is blocked (e.g., LM609 to block $\alpha_v\beta_3$, or P1F6 to block $\alpha_v\beta_5$), but a complete block occurs in the presence of both antibodies (Fig. 4 C). Although the inactive $SSTN_{94-119}$ is without effect even at 100 μM, addition of either 5 μM mS1ED, 0.5 μM $SSTN_{82-130}$, or 0.5 μM $SSTN_{92-119}$ blocks spreading on VN as effectively as (if not better than)

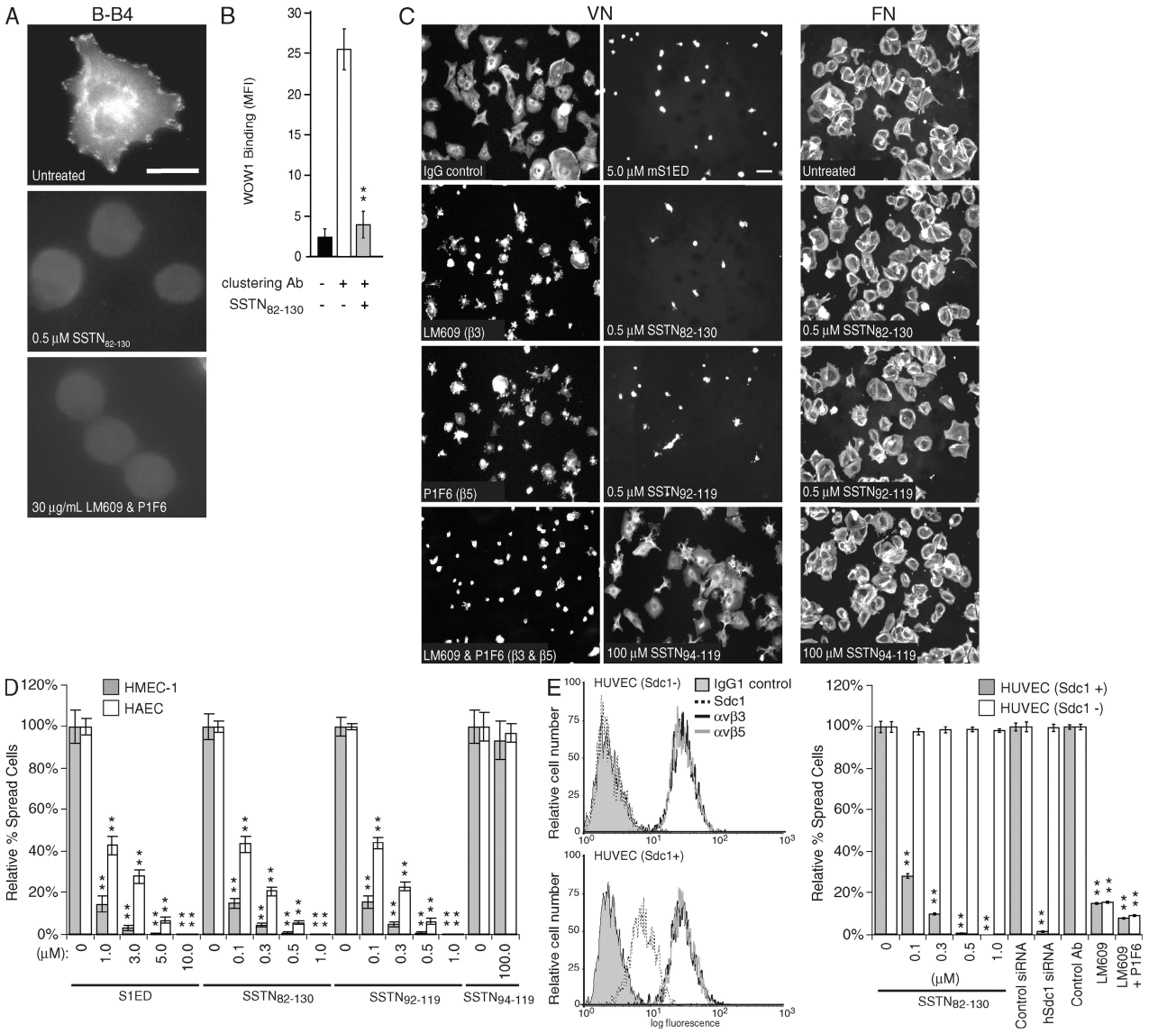

Figure 4. Inhibition of $\alpha_v\beta_3$ and $\alpha_v\beta_5$ integrin activation in HMEC-1 vascular endothelial cells by SSTN. (A) Activation of $\alpha_v\beta_3$ integrin is blocked by SSTN. HMEC-1s plated for 2 h on hSdc1-specific antibody B-B4 in the presence or absence of 0.5 μM $SSTN_{82-130}$ or 30 μg/ml of mAbs LM609 and P1F6. Integrin activation is shown by integrin-dependent cell spreading and by staining with the monovalent ligand-mimetic Fab antibody WOW-1. Results are representative of triplicate wells and two independent experiments. Bar, 20 μm. (B) Integrin activation by Sdc1 clustering. $Sdc1^+$ HUVECs in suspension were treated with mAb B-A38 to engage Sdc1 and was treated with or without secondary antibody to cluster the syndecan in the presence or absence of 1 μM $SSTN_{82-130}$. Quantification of WOW-1 binding via flow cytometry was used to measure the levels of activated $\alpha_v\beta_3$ integrin. Results are representative of duplicate samples and at least two independent experiments. MFI, mean fluorescent intensity. (C) HMEC-1 spreading on VN is dependent on integrins $\alpha_v\beta_3$ and $\alpha_v\beta_5$ and is blocked by SSTN. HMEC-1s plated on VN for 2 h were treated with 30 μg/ml of mAb LM609 ($\alpha_v\beta_3$ blocker), 30 μg/ml of mAb P1F6 ($\alpha_v\beta_5$ blocker), or both antibodies, or 5 μM mS1ED, or 0.5 μM $SSTN_{82-130}$, $SSTN_{92-119}$, or $SSTN_{94-119}$ as competitive inhibitors. The SSTN inhibitors were also tested on cells plated on FN as a negative control (right column). Results are representative of triplicate wells and at least two independent experiments. Bar, 50 μm. (D) Quantification of cell spreading. The percentage of spread HMEC-1s and HAECs was quantified after plating for 2 h on VN in the presence of mS1ED or SSTN peptides. **, $P < 0.01$. (E) Sdc1-negative HUVECs have activated $\alpha_v\beta_3$ and $\alpha_v\beta_5$ integrin but are insensitive to inhibitory SSTN peptide treatment. Expression of Sdc1, $\alpha_v\beta_3$, and $\alpha_v\beta_5$ are quantified by flow cytometry (left) in two isolates of HUVECs, one of which is Sdc1 negative ($Sdc1^-$). The $Sdc1^+$ and $Sdc1^-$ HUVECs are compared in cell spreading assays on VN, using competition with $SSTN_{82-130}$, silencing Sdc1 expression with siRNA, and blocking $\alpha_v\beta_3$ alone or both $\alpha_v\beta_3$ and $\alpha_v\beta_5$ integrins with blocking antibodies LM609 and P1F6 (right). Results are representative of triplicate wells and at least two independent experiments. Data are presented as means ± SEM. **, $P < 0.01$.

the combined antibody treatment (Fig. 4 B). Attachment and spreading on FN is not affected by these peptides (Fig. 4 C) or by the integrin blocking antibodies (unpublished data). Quantification of these results shows that competition with mS1ED at 1–3-μM concentrations reduces HMEC-1 cell spreading on VN by >80–90% (Fig. 4 D), with an ID_{50} of ~1 μM for HAECs, which are more resistant than the HMEC-1s. In comparison, $SSTN_{82\text{-}130}$ and $SSTN_{92\text{-}119}$ display an equivalent inhibitory activity when used at a 10-fold lower concentration, displaying significant inhibitory properties in the 0.1–0.3-μM range. As observed in Fig. 4 C, cell adhesion is also disrupted at the higher inhibitory concentrations and can be prevented altogether by adding increased concentrations of the peptides (unpublished data).

Lastly, the specificity of the SSTN peptides for this Sdc1-regulated mechanism was demonstrated comparing HUVECs that are either positive or negative for Sdc1 expression. Although primary HUVECs do express Sdc1 ($Sdc1^+$), one isolate of these cells that we obtained failed to express the proteoglycan ($Sdc1^-$), as shown by flow cytometry (Fig. 4 E, left); both the $Sdc1^+$ and $Sdc1^-$ cells express identical levels of $\alpha_v\beta_3$ and $\alpha_v\beta_5$ integrins. Somewhat surprisingly, both sets of cells attach and spread on VN (Fig. 4 E, right), both are inhibited by mAb LM609, and both are inhibited further by addition of mAbs LM609 and P1F6 to block both $\alpha_v\beta_3$ and $\alpha_v\beta_5$ integrins. Addition of $SSTN_{82\text{-}130}$ inhibits the spreading of the $Sdc1^+$ HUVECs, similar to its effect on HMEC-1s and HAECs, but is without effect on the $Sdc1^-$ HUVECs. Similarly, silencing Sdc1 expression on the $Sdc1^+$ HUVECs blocks their spreading, whereas the siRNA is without effect on the $Sdc1^-$ cells, as would be expected. This suggests that an alternative activation mechanism exists in the absence of Sdc1 gene expression, and that the SSTN peptide is specific only for the Sdc1-regulated $\alpha_v\beta_3$ and $\alpha_v\beta_5$ activation mechanism.

SSTN inhibits angiogenesis in vitro and in vivo

As a first step in understanding a potential role for Sdc1 in angiogenesis in vivo, we questioned whether Sdc1 was expressed either in the endothelial lining of resting blood vessels (using the mouse aorta) or in microvessels arising from the aorta in response to angiogenic stimuli. As we found when examining the MAEC line in culture (Fig. 3 A), both Sdc1 and the $\alpha_v\beta_3$ and $\alpha_v\beta_5$ integrins are present even on the resting mouse aorta (Fig. 5 A). In addition, microvessels growing out from mouse aortic explants over 7 d in response to FGF-2 stain positively for Sdc1, which appears coexpressed with the $\alpha_v\beta_3$ and $\alpha_v\beta_5$ integrins (Fig. 5 B). In addition, Sdc1 expression is observed in activated endothelial cells of mouse tumor vasculature (Fig. 5 C). Tumors derived from Wnt-1 overexpression (31) in the mammary gland show a high degree of vascularization, identified as internal networks lined by a thick cell layer that stains intensely for Sdc1 and for platelet–endothelial cell adhesion molecule–1 (PECAM-1/CD31), indicative of activated endothelium. In fact, Sdc1 expression in these cells swamps out the positive staining for Sdc1 seen in the mammary epithelial cells, which are known to be Sdc1 positive. These same cell layers are positive for α_v, β_3, and β_5 integrin subunits. A similar finding is seen in mammary tumors arising from overexpression of ΔN89β-catenin (32). Although the vascularization is not as extensive as in the Wnt-1–induced tumors, there are clear thickened layers of activated endothelial cells that are positive for PECAM-1, Sdc1, and $\alpha_v\beta_3/\alpha_v\beta_5$ integrin in these mammary tumors.

To test the importance of the Sdc1 regulatory mechanism during angiogenesis, we tested the activity of SSTN peptides in the in vitro mouse aortic ring outgrowth assay (33) and the in vivo mouse corneal pocket angiogenesis model (34). The aortic outgrowth assay was used to quantify microvessel outgrowth from segments of mouse aorta explanted to collagen gels in the presence of either VEGF or FGF-2, and incubated in the presence of either recombinant mS1ED protein or SSTN peptides. Microvessels are observed growing out of the aortic explants over 7 d in response to VEGF, and this is blocked by increasing concentrations of $SSTN_{82\text{-}130}$ or by an antibody (M9) that inhibits mouse α_v-containing integrins (Fig. 6 A). Single cells observed to be migrating out from the explants in the presence of SSTN or the blocking antibody are likely to be fibroblasts and pericytes. Indeed, desmin staining shows that pericytes line up on the PECAM-positive microvessels in the absence of SSTN and continue to migrate out from the explant in a disorganized fashion when SSTN prevents the outgrowth of PECAM-positive endothelial cells (Fig. 6 B).

Quantification of vessel outgrowth shows that SSTN inhibits both VEGF- and FGF-stimulated outgrowth. Although some vessel outgrowth is observed in the absence of exogenous angiogenic agents, likely caused by VEGF released by the pericytes growing out from the explant (35), the outgrowth is greatly increased by supplementation with FGF-2 or VEGF (Fig. 6, C and D). Addition of recombinant S1ED blocks VEGF-induced outgrowth by >70% at 10 μM and >95% at 30 μM (Fig. 6 C). FGF-induced outgrowth (Fig. 6 D) requires slightly higher inhibitory concentrations (~30 μM mS1ED for 70% inhibition). In comparison, $SSTN_{82\text{-}130}$ and $SSTN_{92\text{-}119}$ are 10–30-fold more potent that mS1ED and show equivalent inhibition of VEGF- or FGF-induced outgrowth, displaying an ID_{50} of ~0.1 μM. These concentrations are nearly identical to the ID_{50}'s displayed in the in vitro cell attachment and spreading assays with HMEC-1s and HAECs (compare with Fig. 4) and are comparable to the effects of 10 μg/ml of the function-blocking α_v integrin mAb M9, which inhibits the activity of both the $\alpha_v\beta_3$ and $\alpha_v\beta_5$ integrins (Fig. 6).

The SSTN peptides were also tested in the in vivo corneal angiogenesis assay (Fig. 7). Poly(2-hydroxyethyl methacrylate) (Poly-HEMA) pellets containing 67 ng FGF-2 and 250 ng sucralfate (used as a slow-release agent) were implanted into the avascular mouse cornea. After 7 d, fluorescent dextran was injected retroorbitally to highlight the vascular system at the time of sacrifice. Visual inspection of either the eye or the dissected cornea shows significant vessel growth toward the implanted pellet from the margin of the cornea. To test the effects of blocking Sdc1, SSTN peptides were delivered systemically via Alzet osmotic pumps (see Materials and methods). Pumps

delivering 1 μl/h of up to 100 μM $SSTN_{82-130}$ or $SSTN_{92-119}$ achieved a nearly total block of angiogenesis, with an ID_{50} of ~3–10 μM (Fig. 7 A; and Fig. 7 C, left). To correlate this with the active concentration in the plasma, we took advantage of rabbit polyclonal antibodies generated against mS1ED that detect active SSTN on dot blots (Fig. 7 B). This shows that SSTN accumulates to 125–150 nM in the blood after 1 wk of treatment with 10 μM SSTN. This correlates well with the ID_{50} of ~100 nM observed in vitro and suggests a clearance rate of 10–13 h in the plasma. In contrast, delivery of 100 μM of the inactive $SSTN_{88-116}$ or $SSTN_{94-119}$ in Alzet pumps has no effect on vessel outgrowth (Fig. 7 A; and Fig. 7 C, left).

We also tested SSTN peptide on male BALB/c Sdc1 knockout mice, as it has been previously reported that angiogenesis is not blocked in this animal (36). Indeed, we found that $Sdc1^{-/-}$ mice display corneal vessel outgrowth in response to FGF-2 (Fig. 7 C, right, blue bars). In addition, this vessel outgrowth is reduced >60% by circulating cRGDfV, a cyclic RGD inhibitory peptide specific for α_v integrins, compared with an inactive cRADfV peptide. This duplicates the extent of inhibition observed for this RGD peptide in other mouse models (15, 37). However, the angiogenesis is not blocked by as much as 100 μM $SSTN_{82-130}$; this concentration of $SSTN_{82-130}$ inhibits angiogenesis by 90% in a parallel

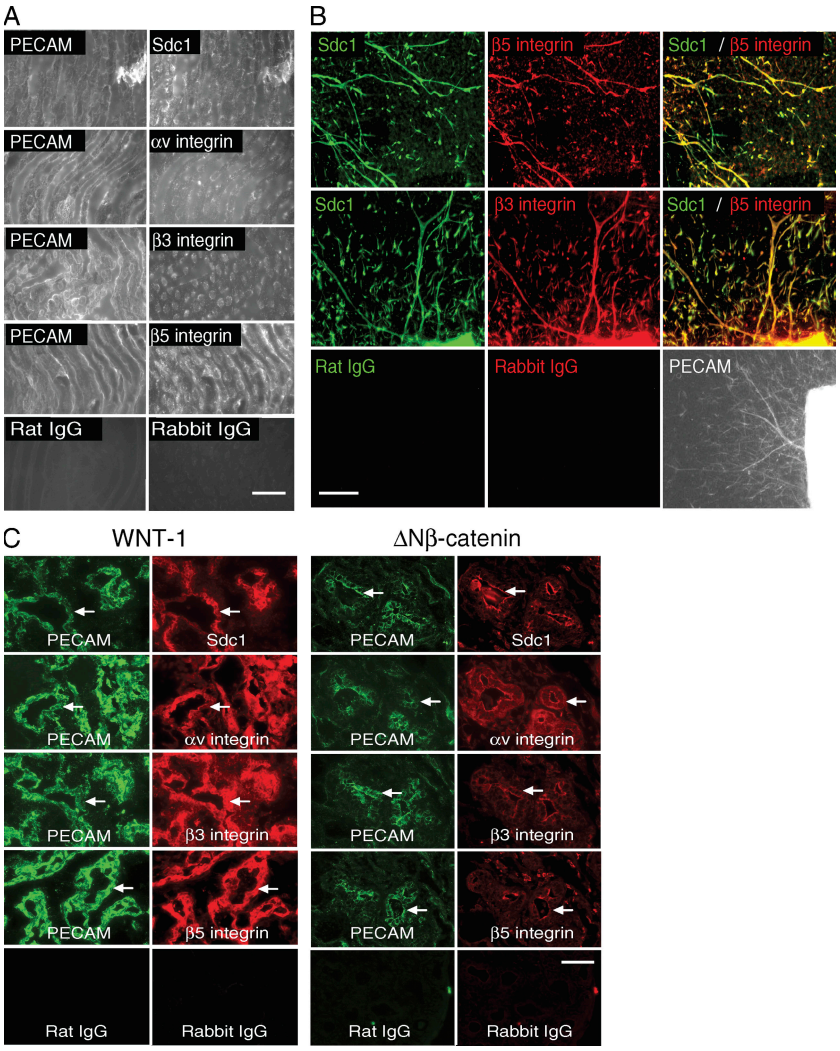

Figure 5. Sdc1 and the $\alpha_v\beta_3/\alpha_v\beta_5$ integrins are coexpressed in normal and tumor vasculature. (A) En face staining of fixed mouse aorta for mSdc1 (mAb 281.2) and mouse α_v (AB1923), β_3 (AB1932), or β_5 (AB1926) integrin subunits. Endothelial cells are present as cords and are identified by mAb 390 (anti-PECAM-1/CD31) staining. Results are representative of at least three independent experiments. Bar, 50 μm. (B) Sdc1 expression in aortic explants. Staining with mSdc1-specific mAb (green) or control rat IgG and β_3 or β_5 integrin–specific IgG (red) or control rabbit IgG in microvessels induced by 30 ng/ml FGF-2 after 7 d from mouse aortic explants grown in type-I collagen gels. PECAM-1 staining of microvessels is also shown. Results are representative of triplicate wells and at least two independent experiments. Bar, 50 μm. (C) Expression of Sdc1 and integrins in tumor vasculature. PECAM-1, Sdc1, or α_v, β_3, or β_5 integrin subunits are stained in frozen sections of spontaneous mammary tumors arising in mice because of MMTV promoter–driven expression of ectopic Wnt-1 or ΔN89β-catenin (three mice each). Arrows point to identical structures in the PECAM and Sdc1 or integrin costained panels to orient the reader. Results are representative of at least three independent experiments. Bar, 50 μm.

experiment with wild-type BALB/c mice (Fig. 7 C, right, red bars). Thus, a compensatory mechanism exists for the activation of the $\alpha_v\beta_3$ and $\alpha_v\beta_5$ integrin in the Sdc1$^{-/-}$ mouse that is insensitive to the inhibitory SSTN peptide.

Finally, $SSTN_{82-130}$ was tested in an in vivo orthotopic tumor model (Fig. 8). MDA-MB-231 human mammary carcinoma cells were injected subcutaneously into female, athymic BALB/c nude mice. Palpable tumors were allowed to form for 1 wk after injection, at which time Alzet pumps delivering 0.25 µl/h of either PBS alone (control) or $SSTN_{82-130}$ were implanted. Tumor growth was monitored for an additional 4 wk before sacrifice. Treatment with 120 µM (0.37 ± 0.02 µM in the serum; not depicted) or 400 µM (1.87 ± 0.06 µM in the serum; not depicted) $SSTN_{82-130}$ results in a significant reduction in tumor size relative to control mice (Fig. 8, A and B). Moreover, staining the tumor sections for PECAM-1 or desmin shows a significant reduction in the number of tumor vessels in the SSTN-treated tumors; both endothelial cells and pericytes are observed, but in reduced numbers of vessels (Fig. 8 C). Quantification of angiogenesis either by measuring total vessel length in the sections or total PECAM-1 positive staining shows an 11-fold reduction in animals bearing pumps containing 400 µM SSTN (Fig. 8 D).

DISCUSSION

Previous work described a dependence on Sdc1 for activation of the $\alpha_v\beta_3$ and $\alpha_v\beta_5$ integrins. This raises the question

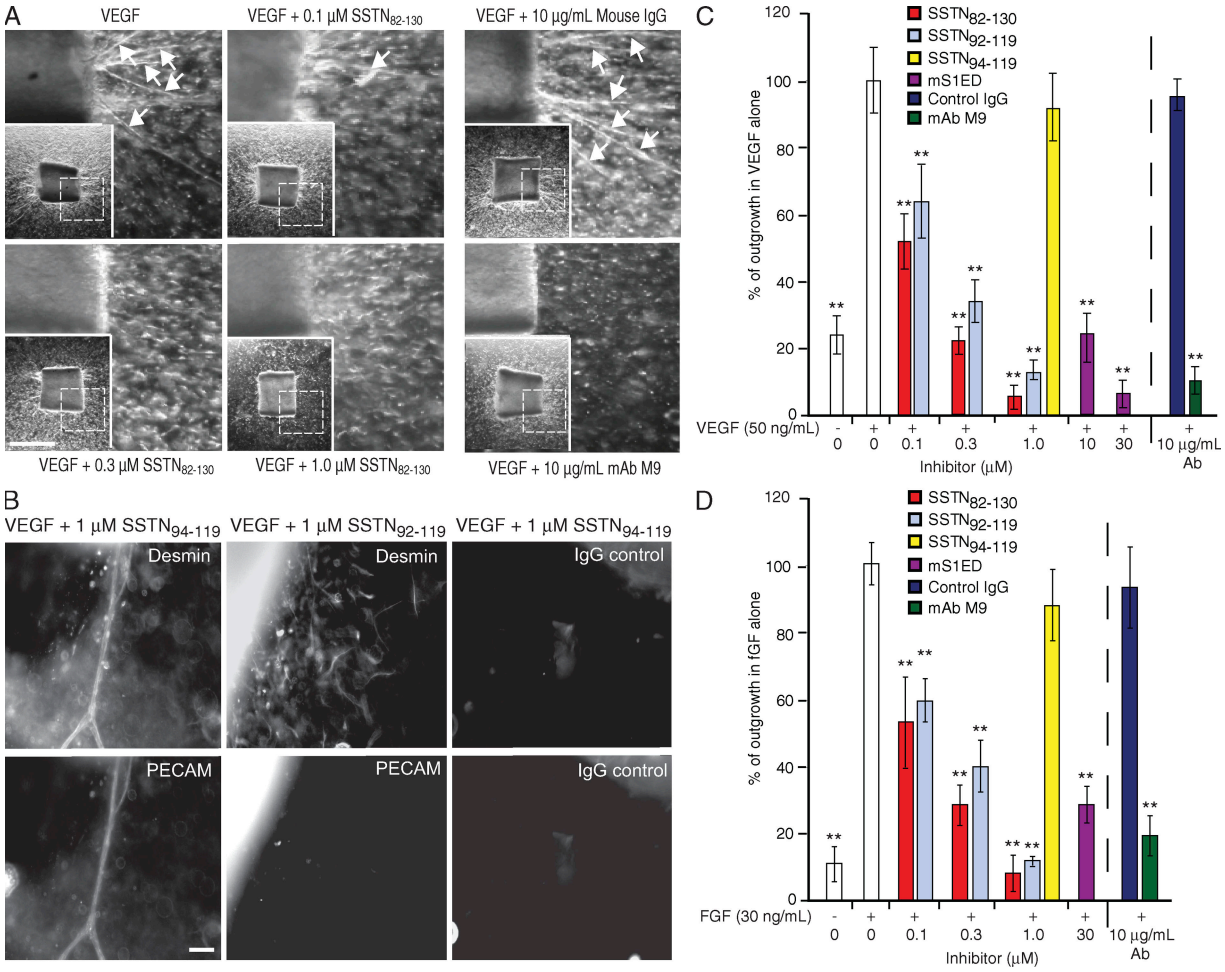

Figure 6. SSTN blocks microvessel outgrowth from mouse aortic explants. (A) Blockade of VEGF-induced outgrowth by SSTN or α_v integrin blocking antibody. Aortic explants to type-I collagen are treated with 50 ng/ml VEGF for 7 d in the presence of 0, 0.1, 0.3, and 1 µM $SSTN_{82-130}$ or 10 µg/ml α_v blocking antibody M9 or a mouse IgG control. Arrows denote microvessels. Insets show full aortic ring with dashed box to identify the magnified area shown. Bar, 0.5 mm. (B) Outgrowth of pericytes and endothelial cells. Aortic rings grown as in A in the presence of $SSTN_{94-119}$ (inactive) or $SSTN_{92-119}$ (active) are stained with rat anti–PECAM-1 (or nonspecific rat IgG) to mark endothelial cells, or mouse anti-desmin (or nonspecific mouse IgG) to identify pericytes. Note that SSTN affects endothelial but not pericyte outgrowth. Bar, 50 µm. (C and D) Quantification of total microvessel outgrowth in VEGF-treated (C) and FGF-treated (D) rings. The total microvessel outgrowth is compared for rings treated with 50 ng/ml VEGF or 30 ng/ml FGF. Each bar represents the total microvessel outgrowth per explant for six explants (±SD). Rings were incubated in medium containing either no addition, mouse S1ED, SSTN peptides, mAb M9, or control mouse IgG. Results are representative of at least three independent experiments. **, $P < 0.01$.

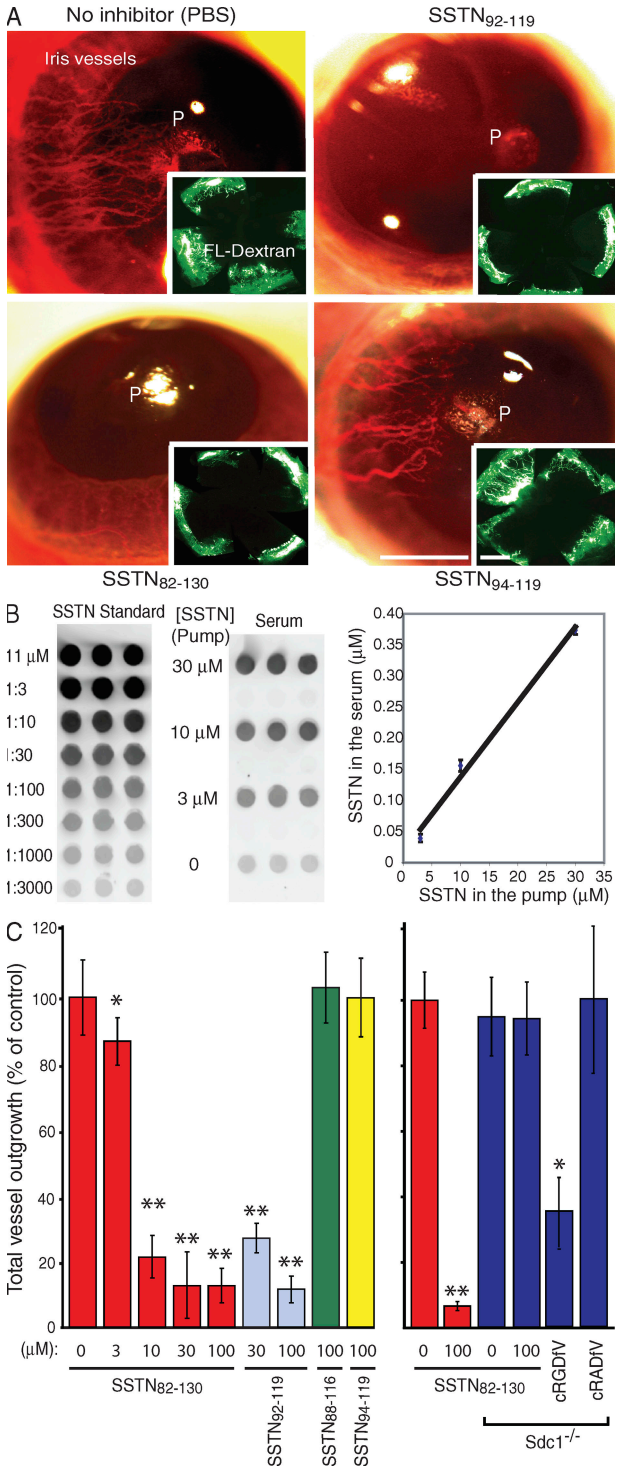

Figure 7. SSTN blocks FGF-induced corneal angiogenesis in vivo. (A) Angiogenic outgrowth in response to FGF. 0.125 µl of Poly-HEMA pellets (P in the images) containing 67 ng FGF-2 and 250 ng sucralfate were implanted in the avascular mouse cornea for 7 d. Alzet osmotic pumps were implanted subcutaneously on the backs of the animals and deliver 1 µl/h PBS or PBS plus 30 µM $SSTN_{82-130}$, $SSTN_{92-119}$, or $SSTN_{94-119}$. Fluorescent dextran is injected intravenously 1–2 min before sacrifice, and angiogenesis is imaged either in the intact eye or by fluorescence of blood vessels in the dissected cornea (insets). Vessels in the iris can be observed but can be distinguished from angiogenesis in the cornea. Results are representative of at least six mice per treatment condition. The experiment was repeated independently three times. Bars, 1 mm. (B) $SSTN_{82-130}$ concentration in the serum. 11 µM $SSTN_{82-130}$ was spotted in triplicate on nitrocellulose with threefold dilutions, detected with Sdc1 polyclonal rabbit antibody (left), and compared with undiluted mouse serum derived from mice treated with 30, 10, 3, or 0 µM $SSTN_{82-130}$ in PBS (middle). The estimated concentration of SSTN in the serum is plotted versus its starting concentration in the pump (right). Data are representative of three independent experiments. (C) Quantification of corneal angiogenesis in wild-type and Sdc1-null ($Sdc1^{-/-}$) mice. Mean total vessel outgrowth in the presence or absence of SSTN (concentration in the pump is shown) is quantified and expressed relative to the PBS control set at 100% (±SD). Wild-type and $Sdc1^{-/-}$ mice (six mice per data point for each cohort from three independent experiments) were directly compared using treatments of 100 µM $SSTN_{82-130}$. The $Sdc1^{-/-}$ mice (three mice per data point for one experiment) were also treated with 22.7 mM α_v integrin–specific cRGDfV inhibitory peptide or inactive cRADfV peptide. Data are presented as means ± SEM. *, $P < 0.05$; **, $P < 0.01$.

of whether this regulatory mechanism exists on the vascular endothelium during angiogenesis. Although expression of Sdc1 in the vascular endothelium has not been studied extensively, several reports indicate that it is expressed in the endothelium of newly formed vessels in wound granulation tissue (38–41) and the endothelial lining of intramyocardial blood vessels in the rat heart (42); however, no expression is seen in blood vessels in unwounded skin (39) nor in the normal rabbit aorta (43), suggesting that its expression may be regulated, perhaps by ephrin signaling (44). A role in angiogenesis, however, is seemingly cast in doubt by the finding that angiogenesis is not impeded in the Sdc1-null mouse (36).

Our findings suggest that Sdc1 is indeed expressed in the vascular endothelium and that its core protein has an important regulatory role during the angiogenic process. It is detected, along with the $\alpha_v\beta_3$ and $\alpha_v\beta_5$ integrins, in cultured MAECs, in resting mouse aorta, and in angiogenic aortic microvessels in vitro and tumor vasculature in vivo. Although we have not investigated directly whether or not Sdc1 expression is up-regulated during angiogenesis, it does display intense staining in the endothelial cells undergoing angiogenesis in the aortic ring outgrowth assay and in mammary tumors. Up-regulated expression of Sdc1 would mimic that of the $\alpha_v\beta_3$ integrin, which displays low or nonexistent expression in most adult tissues and is dramatically up-regulated in the vascular endothelium during angiogenesis (45–47). Most importantly, blocking Sdc1 expression or competitively blocking its interaction with these integrins using SSTN serves to inactivate the integrins and block endothelial cell attachment, spreading, and invasion/outgrowth in vitro, as well as angiogenesis and tumor growth in vivo. The regulatory mechanism remains unknown, but it appears to rely on a direct interaction between the integrins and Sdc1.

Interestingly, our findings do confirm the ability of the Sdc1-null mouse to mount a seemingly normal angiogenic response, a response that appears dependent on the $\alpha_v\beta_3$ and $\alpha_v\beta_5$ integrins despite the absence of Sdc1. This finding is

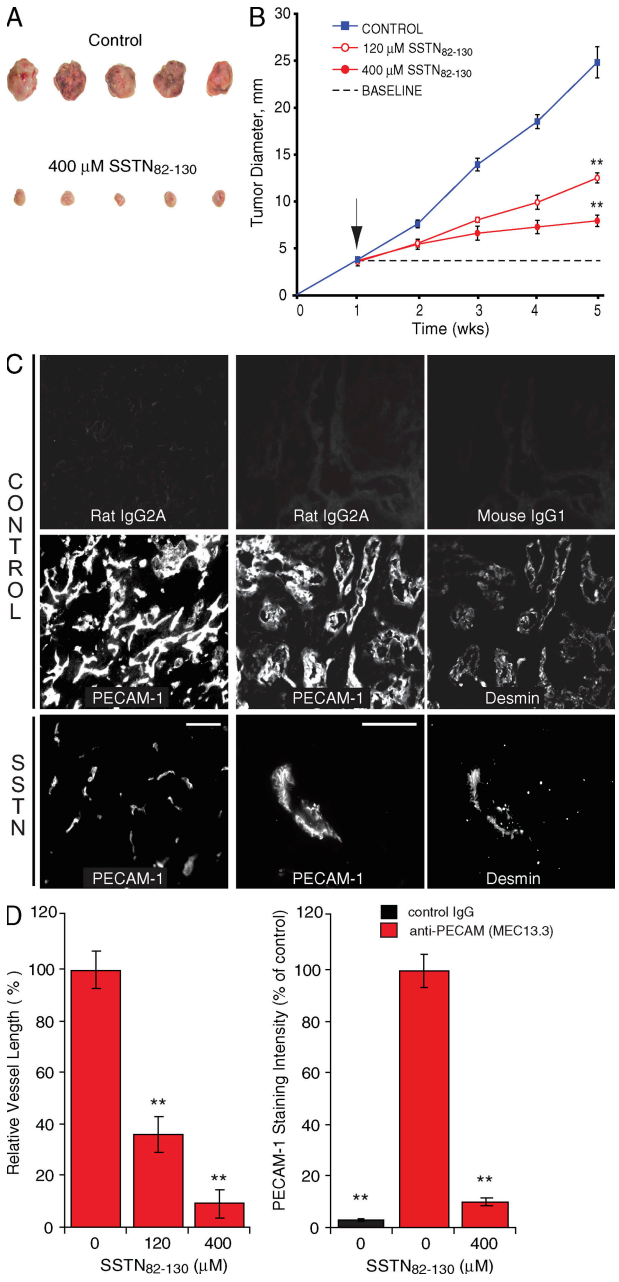

Figure 8. Inhibition of tumor growth by SSTN. (A) Effects of SSTN on tumor growth. Isolated 5-wk-old tumors from female BALB/c nude mice bearing Alzet pumps delivering PBS or PBS plus 400 μM $SSTN_{82-130}$. (B) Quantification of tumor growth over time. Alzet pumps containing PBS, or PBS with 120 μM or 400 μM $SSTN_{82-130}$ were implanted on the flank of nude mice with 1-wk-old subcutaneous MDA-MB-231 cell tumors (arrow and baseline tumor size). Tumor size was measured at weekly intervals for 4 wk of each ensuing treatment. **, $P < 0.01$. (C) Detection of tumor vasculature in frozen OCT-embedded sections. Sections are stained with anti–PECAM-1 (mAb MEC 13.3) or nonspecific rat IgG2A and Alexa Fluor 488–conjugated goat anti-rat secondary antibody to detect endothelial cells, and anti-desmin or nonspecific mouse IgG1 and Alexa Fluor 546–conjugated secondary antibody to detect pericytes. Bars, 50 μm. (D) Quantification of total PECAM-positive vessels. Relative angiogenesis was quantified by totaling either vessel length (left) or total PECAM-1 staining intensity (right) in frozen sections of tumors from mice treated with or without $SSTN_{82-130}$. Data are from two independent experiments with a minimum of six mice per data point in each, and are presented as means ± SEM. **, $P < 0.01$.

matched by an isolate of HUVECs that are also Sdc1 negative. They display active $\alpha_v\beta_3$ and $\alpha_v\beta_5$ integrins, but unlike their Sdc1-positive counterparts, they are not dependent on Sdc1 and are unaffected by SSTN. In these Sdc1-negative cells (and in the Sdc1-null mice), integrin activation presumably occurs via a compensatory mechanism that is activated in the absence of Sdc1 gene expression. This not only explains why angiogenesis is observed in the Sdc1-null mouse, but it also provides a strong argument for the specificity of the SSTN peptide. That is, the peptide appears to compete for a specific interaction of Sdc1 with these integrins that is essential for their activation on Sdc1-expressing cells. If this mechanism is absent, the peptide has no apparent off-target effects even at concentrations up to 100-fold greater than its ID_{50}.

Although the mechanisms of integrin activation have received considerable scrutiny, especially during processes such as platelet activation and in angiogenesis, the reliance of the $\alpha_v\beta_3$ and $\alpha_v\beta_5$ integrins on Sdc1 during angiogenesis has not been appreciated until now. The $\alpha_v\beta_3$ integrin has been shown previously to associate with other membrane proteins, with some leading to enhanced activation of the integrin (48). Integrin-associated protein (also known as CD47) presents an intriguing comparison to Sdc1 in that it associates with the $\alpha_{IIb}\beta_3$ and $\alpha_v\beta_3$ integrins via its extracellular domain, and this interaction alone is sufficient to activate these integrins (49, 50).

The activation of an integrin typically refers to a conformation change that dramatically increases ligand binding affinity, and the $\alpha_{IIb}\beta_3$ and $\alpha_v\beta_3$ integrins have been used as models to begin to understand the activation mechanism. It proceeds through two or more activation states, each resulting in a conformational change in the integrin's extracellular domain in response to intracellular signals and extracellular ligand binding (51–55). In a current model for $\alpha_v\beta_3$ activation, the inactive integrin is in a bent configuration and opens like a switchblade when activated (56). This occurs in response to talin binding to the β_3 integrin cytoplasmic domain and breaking of the salt bridge that maintains the inactive conformation (57, 58). However, it is also enhanced by oligomerization of the integrin subunits within the plane of the plasma membrane (59), and by extracellular interactions with matrix ligands and/or other membrane proteins (48).

Our data now suggest that the active conformation of the $\alpha_v\beta_3$ and $\alpha_v\beta_5$ integrins is favored by their direct association with Sdc1. The integrins are activated by plating endothelial cells on Sdc1 antibody, or by antibody-induced clustering of Sdc1 on suspended endothelial cells, as shown in this study by the binding of the ligand-mimetic Fab WOW-1; this has also been shown with carcinoma cells (20). The activation that occurs when Sdc1 is engaged by antibody is not blocked by depletion of divalent cations that are otherwise necessary for

ligand binding by the integrin, indicating that Sdc1 is engaged as a membrane coreceptor, not as a ligand. The fact that WOW-1 is a monovalent Fab indicates that the activation is a true increase in integrin affinity rather than increased avidity. As we now show that the syndecan and $\alpha_v\beta_3$ and/or $\alpha_v\beta_5$ integrins form a complex, likely via lateral interactions of their extracellular domains, it seems apparent that clustering Sdc1 leads to clustering of the integrins as well. It is possible that the clustering brings together kinases associated either with the integrin or the Sdc1, initiating kinase transphosphorylation and activation of signaling pathways that activate the integrin through talin. In vivo, clustering would be envisioned to take place when Sdc1 engages the heparin-binding domains of multivalent matrix ligands. SSTN appears to inhibit tumorigenesis and angiogenesis by displacing Sdc1 from the integrins and, thus, blocking their activation during this clustering event.

MATERIALS AND METHODS

Materials. Sdc1-specific antibodies used were mouse mAbs B-B4 and B-A38 (hSdc1; AbD Serotec) and rat mAb 281.2 (mSdc1) (60). Rabbit polyclonal antibodies against recombinant mS1ED were affinity purified as previously described (20) and used to detect SSTN. Mouse mAb 3G10, which specifically recognizes terminal unsaturated uronic acid residues that remain on the core protein after treatment with heparin lyases (61), was used for simultaneous detection of mSdc1 and hSdc1 on Western blots. Integrin antibodies include the polyclonal antibodies AB1923, AB1932, and AB1926 (against α_v, β_3, and β_5, respectively; Millipore) and mAb N29 (used for Western blotting for β_1; Millipore); blocking mAbs P1F6 and M9 (for $\alpha_v\beta_5$ and α_v, respectively; Millipore), LM609 (for $\alpha_v\beta_3$; courtesy of D. Cheresh, University of California, San Diego, La Jolla, CA, and the Scripps Research Institute, La Jolla, CA); and "Fire & Ice" (rabbit anti-β_3; courtesy of P. Newman, Blood Research Institute, Blood Center of Southeastern Wisconsin, Milwaukee, WI). Mouse $\alpha_v\beta_5$ ALULA function-blocking mAb was provided courtesy of D. Sheppard (University of California, San Francisco, San Francisco, CA). WOW-1, a ligand-mimetic Fab that serves as an "activation sensor" for $\alpha_v\beta_3$, was provided courtesy of S. Shattil (University of California, San Diego, La Jolla, CA) (30). Rat mAbs MEC 13.3 (BD) or 390 (Millipore) against mouse CD31/PECAM-1 were used to identify endothelial cells. Mouse mAb D33 (Dako) against desmin was used to identify pericytes.

Mouse mammary tumors were provided by C. Alexander (University of Wisconsin-Madison, Madison, WI); tumors were from mice overexpressing Wnt-1 under control of the MMTV-LTR (31, 62) or from FVB MMTV–ΔN89β-catenin transgenic mice (63). Tumors were embedded in optimum cutting temperature (OCT) compound (VWR) and frozen sections were prepared for staining.

The SSTN peptides (80–90% pure) were purchased from GenScript Corporation. They are based on the mSdc1 sequence. Recombinant mS1ED fusion protein was prepared as previously described (20).

Type-I collagen was purified from rat tail tendons (64), solubilized in 0.1 M acetic acid, and dialyzed against 0.1× DMEM (no serum) at pH 4 to remove the acetic acid. VN was purified from human plasma using a previously described method (65).

Cell culture. All cell lines were cultured at 37°C in 92.5% air/7.5% CO_2. MDA-MB-231 human mammary carcinoma cells and MAECs were grown in DMEM (Thermo Fisher Scientific) supplemented with 10% FCS (Thermo Fisher Scientific), 4 mM L-glutamine (Sigma-Aldrich), and 100 U/ml penicillin and 100 μg/ml streptomycin (Invitrogen). MAECs and HAECs were provided by R. Auerbach (University of Wisconsin-Madison, Madison, WI). These are spontaneously immortalized cell lines identified as endothelial by phenotypic markers (66). SV40-T immortalized HMEC-1s were developed and provided by E.W. Ades and F.J. Candal (Center for Disease Control, Atlanta, GA) and T.J. Lawley (Emory University, Atlanta, GA) (67). HUVECs were obtained from Cambrex Life Sciences Corp. Human endothelial cells were cultured in MCDB-131 (Invitrogen) medium supplemented with 5 mM L-glutamine, 20 mM $NaHCO_3$ (Sigma-Aldrich), 10 ng/ml epidermal growth factor, 1 μg/ml hydrocortisone, bovine brain extract with heparin and antibiotics (SingleQuot kit; Cambrex Life Sciences Corp.), and 15% FBS (Gemini Bio-Products).

Cell attachment and spreading assay. Cell attachment and spreading assays on Sdc1-specific antibody or VN and silencing of Sdc1 expression by siRNA were conducted as previously described (19, 20). *Silencer* control siRNAs (Applera Corporation) were use for control siRNA transfections. Images were acquired using an objective (PlanFluor 10× [0.5 NA], PlanApo 20× [0.75 NA], or PlanApo 63× [1.4 NA]; Nikon) on a microscope (Microphot-FX; Nikon) equipped with a cooled charge-coupled device camera system (Image-Point; Nikon).

Construction of mSdc1 mutant. The $mSdc1^{\Delta 67-121}$ mutant was constructed by digesting full-length mSdc1 cDNA (pcDNA3; provided by R. Sanderson, University of Alabama at Birmingham, Birmingham, AL) with BmgBI and BstEII. The BstEII overhang was then filled in using the Klenow DNA polymerase fragment (Promega) and the vector then blunt-end ligated using T4 DNA ligase (New England Biolabs, Inc.). The mutant was transfected into MDA-MB-231 cells using LipofectAMINE PLUS (Invitrogen) and 10 μg of plasmid, in accordance with the manufacturer's instructions. A stable population (100–300 colonies) was selected in 1.5 mg/ml G418 (EMD) and comparatively sorted against cells expressing full-length mSdc1 for equal expression levels by flow cytometry using mAb 281.2 under sterile conditions on a triple-laser FACSVantage SE equipped with a FACSDiva digital electronics analyzer (BD).

Flow cytometry. Cells were scanned at the University of Wisconsin Comprehensive Cancer Center Flow Cytometry Facility using a benchtop cytometer (FACSCalibur; BD Biosciences). For cell-surface staining of Sdc1 and/or integrins, cells were lifted in Tris-buffered saline (TBS) containing 5mM EDTA (TES), washed in HEPES-buffered DMEM (Hb-DME) containing 10% serum, incubated for 1 h on ice with 1 μg of primary antibody per 5×10^5 cells, washed, and counterstained with Alexa Fluor 488–conjugated secondary antibodies (Invitrogen). Cell scatter and propidium iodide (1 μg per sample; Sigma-Aldrich) staining profiles were used to gate live, single-cell events for data analysis. For WOW1 Fab staining (i.e., detection of activated $\alpha_v\beta_3$ integrin), HUVECs were lifted in TES and washed in serum-free medium (Hb-DME containing 0.1% heat-denatured BSA [hdBSA]); this medium was used for all washes and incubations that follow unless otherwise specified. To cluster Sdc1, suspended cells were incubated with 1 μg/ml of mAb B-A38 per 5×10^5 cells (or mIgG1 as an isotype control) for 15 min at 37°C, washed, and incubated with 5 μg/ml goat anti–mouse IgG secondary antibody (Jackson ImmunoResearch Laboratories) for an additional 15 min. Cells were washed and blocked for 15 min in serum-free medium containing 1% hdBSA and a 1:100 dilution of monovalent Fab fragment of goat anti–mouse IgG. Cells were washed with a stoichiometric excess of serum-free medium and incubated with WOW-1 Fab (1:4 dilution) for 30 min at 37°C in the presence or absence of 1 μM $SSTN_{82-130}$. Cells were washed with serum-free medium, fixed in 4% paraformaldehyde (PFA) for 30 min, and quenched in 0.1 M glycine (in PBS) for 15 min. Cells were then counterstained with 10 μg/ml Alexa Fluor 488–conjugated goat anti–mouse IgG secondary antibody (Invitrogen) before scanning. Mean fluorescent intensity of triplicate samples was used as a measure of activated $\alpha_v\beta_3$ integrin.

Immunoprecipitations. mSdc1 and hSdc1 were immunoprecipitated using mAbs 281.2 and B-B4, respectively. $3–5 \times 10^6$ cells per milliliter were washed and lysed in buffer containing 50 mM HEPES (pH 7.4), 150 mM NaCl, 10 mM EDTA, 1% Triton X-100, 0.5% sodium deoxycholate, and a 1:100 dilution of protease inhibitor cocktail set III (EMD) for 20 min on ice. Insoluble cell debris was removed by centrifugation at 20,000 *g* for 15 min at 4°C. Cell

lysates (2-mg input determined by BCA assay per reaction; Thermo Fisher Scientific) were precleared using 50 μg/ml of isotype-matched IgG (rat IgG2A for 281.2 and mouse IgG1 for B-B4) and 100 μl of GammaBind Sepharose (50:50 bead/lysis buffer slurry; GE Healthcare). Precleared lysates were incubated at 4°C overnight with 10 μg/ml of anti-syndecan antibody. For competition experiments, 30 μM GST (negative control), 30 μM GST-S1ED, or 3 μM SSTN was added to the precleared lysates in conjunction with anti-Sdc1 antibody. Immune complexes were precipitated with GammaBind Sepharose, pelleted, washed, and incubated in 50 μl of heparitinase buffer (50 mM Hepes, 50 mM NaOAc, 150 mM NaCl, and 5 mM $CaCl_2$ [pH 6.5]) containing 2.4×10^{-3} IU/ml heparitinase (IBEX Technologies, Inc.) and 0.1 conventional U/ml of chondroitin ABC lysase (ICN Biochemicals) for 4 h at 37°C (with fresh enzymes added after 2 h) to remove glycosaminoglycan side chains from the immunoprecipitated syndecan. For precipitations using purified components, GST or GST-S1ED protein was immobilized to glutathione agarose beads (GE Healthcare) and incubated with either purified $\alpha_v\beta_3$ or $\alpha_v\beta_5$ integrin (U.S. Biological) in the presence of either competitive $SSTN_{92\text{-}119}$ or noncompetitive $SSTN_{94\text{-}119}$ peptide in sterile PBS containing the protease inhibitor cocktail for 4 h at 4°C. The samples were pelleted and washed in sterile PBS. In biotin label transfer assays, SSTN "bait" (active peptide 92–119 or inactive peptide 94–119) was labeled with Sulfo-SBED Biotin (Thermo Fisher Scientific) in accordance with the manufacturer's instructions and incubated with purified $\alpha_v\beta_3$ integrin "prey" protein in solution. The SBED conjugate was photoactivated with UV light (365 nm at 5 cm for 15 min) to cross-link the bait–prey complexes. After reversal of the cross-links with dithiothreitol, biotin-labeled prey protein was captured using monomeric avidin agarose beads (Thermo Fisher Scientific). All samples were extracted in Laemmli sample buffer (68) and resolved by electrophoresis on a 7.5% Laemmli gel, transferred to ImmobilonP, and probed with alkaline phosphatase (AP)–conjugated streptavidin alone, or 10 μg/ml rabbit anti-β_3 Fire & Ice, rabbit polyclonal anti-β_5 integrin (1:1,000), 10 μg/ml mouse anti–human α_v mAb 3F12 (courtesy of S. Blystone, State University of New York Upstate Medical University, Syracuse, NY), or 1 μg/ml polyclonal anti–mouse S1ED or mAb B-A38 antibody followed by an AP-conjugated secondary. Visualization of immunoreactive bands was performed using ECF reagent (GE Healthcare) and scanned on a Storm PhosphoImager (GE Healthcare).

Aortic ring outgrowth assay. All animal experiments were approved by the University of Wisconsin Institutional Animal Care and Use Committee. Mouse aortic ring outgrowth assays were conducted as in Masson et al. (33). The thoracic aortae from female BALB/c mice were cut into 1-mm segments and placed in 1.6-mg/ml collagen gels containing MCDB-131 endothelial cell growth medium (Invitrogen) and fresh 2.5% mouse serum, 100 U/ml penicillin, and 100 μg/ml streptomycin. Media containing 30 ng/ml FGF-2 (PeproTech) or 50 ng/ml VEGF (PeproTech) and recombinant mS1ED or SSTN peptide was changed every 2 d for the duration of the experiment (7 d). Total vessel outgrowth was summed for each ring using Metamorph software (version 6.1; MDS Analytical Technologies). Immunofluorescent images were acquired using a PlanApo 20× (0.75 NA) objective and a camera (CoolSnap ES; Roper Scientific) on a microscopy system (Eclipse TE2000U; Nikon). Digital images were acquired using a dissecting microscope (SMZ1500; Nikon) and a digital camera (CoolPix E5000; Nikon).

Corneal angiogenesis assay. For corneal angiogenesis, pellets were created using 3 vol Poly-HEMA (Sigma-Aldrich) in 95% ethanol, and 1 vol each of sucralfate (100 μg/ml in PBS; Sigma-Aldrich), FGF-2 (3.2 mg/ml in PBS; PeproTech), and PBS. The solution was rapidly mixed, and 0.5-μl drops were allowed to dry for 1 h at 4°C before being cut into four equal 0.125-μl sections for implantation into corneal pockets created in anesthetized mice using a 1.5-mm microdissecting knife (Roboz Surgical Instrument Company, Inc.). Osmotic pumps (model 2004; Alzet Osmotic Pumps) delivering 1 μl/h containing PBS or PBS with a range of SSTN concentrations from 0–100 μM, or PBS containing 22.7 mM cRGDfV or cRADfV peptide (Enzo Life Sciences, Inc.), reconstituted in a 50:50 DMSO/double-distilled H_2O solution, were implanted immediately after pellet implantation. After 7 d, 0.1 ml FITC-dextran (2,000,000 mol wt; Sigma-Aldrich) was retro-orbitally injected into each mouse before sacrifice, and corneas were removed and fixed in 4% PFA for imaging. Total vessel outgrowth from the limbic vessel at the cornea margin was summed for each mouse using Metamorph software. Immunofluorescent images were acquired using a PlanFluor 4× (0.45 NA) objective and a CoolSnap ES camera on an Eclipse TE2000U microscopy system. Digital images were acquired using a SMZ1500 dissecting microscope and a CoolPix E5000 digital camera.

Subcutaneous tumors. Under aseptic conditions, 5×10^6 MDA-MB-231 human mammary carcinoma cells (0.2 ml vol) were injected subcutaneously in the right rear flank of 6–8-wk-old female, athymic BALB/c nude mice (Taconic) using a 3-ml sterile syringe and a 26-gauge needle. Palpable tumors were allowed to form for 1 wk after injection, at which time each animal was surgically implanted with an Alzet osmotic pump (0.25 μl/h) containing either PBS (control) or PBS plus $SSTN_{82\text{-}130}$ peptide (either 120 or 400 μM). Tumor growth was monitored for an additional 4 wk by weekly examination and caliper measurements. At 5 wk after injection, the mice were humanely sacrificed and tumors/serum were harvested.

5–8-μm serial sections cut from frozen, OCT-embedded tumors were periodate-lysine-paraformaldehyde fixed, quenched in 0.05% $NaBH_4$ followed by 0.1M glycine, and permeabilized/blocked in IHC buffer (0.02% NaN3, 0.1% BSA, 0.2% Triton X-100, and 0.05% Tween 20 in PBS) containing 10% goat serum. Sections were stained with rat anti–mouse PECAM-1/CD31 mAb MEC 13.3 (1:25 dilution in IHC buffer) and/or mouse anti-desmin (used neat) followed by Alexa Fluor 488–conjugated goat anti–rat/mouse secondary antibody. Images were acquired using a PlanFluor 40× objective (1.3 NA; Nikon) and a CoolSnap ES camera on an Eclipse TE2000U microscopy system. Mean vessel length and PECAM-1 staining intensity were calculated across six representative fields for each cohort (i.e., control vs. SSTN-treated mice) using Metamorph software.

Dot blots. SSTN serum levels were calculated by dot blotting using affinity-purified, rabbit polyclonal anti-S1ED antibody. In brief, mouse serum collected from SSTN-treated and control mice was pooled and heated at 65°C for 20–30 min (to inactivate endogenous AP activity), and 200 μl was spotted in triplicate on 0.2 μm nitrocellulose (Bio-Rad Laboratories) using a vacuum (Minifold Dot-Blot System; Schleicher & Schuell). After washing, the membrane was fixed in 0.25% glutaraldehyde for 30 min, blocked in TBS containing 6% BSA for 2 h at 4°C, and then probed using 1 μg/ml anti-S1ED antibody followed by AP-conjugated donkey anti–rabbit secondary antibody (1:5,000 dilution). Immunoreactive wells were visualized using ECF reagent and scanned on a Storm PhosphoImager. SSTN levels were calculated using Image Quant software (GE Healthcare) by comparison against a standard curve (i.e., 0–18 μM SSTN-spiked, heat-inactivated serum collected from control mice) spotted on the same blot.

Statistical analyses. Statistical analyses using a two-tailed Student's *t* test were performed using Prism software (version 5; GraphPad Software, Inc.). Data that satisfy confidence levels of $P < 0.05$ or 0.01 are noted. Data are presented as means ± SEM, unless otherwise noted.

Drs. D. Cheresh and S. Shattil, C. Alexander and R. Auerbach, P. Newman, D. Sheppard, S. Blystone, and R. Sanderson are thanked for generously providing cells, tissues, and/or reagents used in this work. G. Thomas is thanked for technical assistance, and Dr. R. Sanderson is thanked for critically reading the manuscript.

This work was supported by funds to A.C. Rapraeger from the National Institutes of Health (grants R01-CA109010 and CA118839) and the American Heart Association (grant AHA0655734Z), and the Robert Draper Technology Innovation Fund of the University of Wisconsin. D.M. Beauvais is supported by a Susan G. Komen Foundation postdoctoral fellowship.

The authors have no conflicting financial interests.

Submitted: 12 June 2008
Accepted: 5 February 2009

REFERENCES

1. Folkman, J. 2006. Angiogenesis. *Annu. Rev. Med.* 57:1–18.
2. Hynes, R.O. 2007. Cell-matrix adhesion in vascular development. *J. Thromb. Haemost.* 5(Suppl. 1):32–40.
3. Stupack, D.G., and D.A. Cheresh. 2003. Apoptotic cues from the extracellular matrix: regulators of angiogenesis. *Oncogene.* 22:9022–9029.
4. Friedlander, M., P.C. Brooks, R.W. Shaffer, C.M. Kincaid, J.A. Varner, and D.A. Cheresh. 1995. Definition of two angiogenic pathways by distinct alpha(v) integrins. *Science.* 270:1500–1502.
5. Stupack, D.G., X.S. Puente, S. Boutsaboualoy, C.M. Storgard, and D.A. Cheresh. 2001. Apoptosis of adherent cells by recruitment of caspase-8 to unligated integrins. *J. Cell Biol.* 155:459–470.
6. Brooks, P.C., R.L. Klemke, S. Schon, J.M. Lewis, M.A. Schwartz, and D.A. Cheresh. 1997. Insulin-like growth factor receptor cooperates with integrin alpha v beta 5 to promote tumor cell dissemination in vivo. *J. Clin. Invest.* 99:1390–1398.
7. De, S., J. Chen, N.V. Narizhneva, W. Heston, J. Brainard, E.H. Sage, and T.V. Byzova. 2003. Molecular pathway for cancer metastasis to bone. *J. Biol. Chem.* 278:39044–39050.
8. Felding-Habermann, B., E. Fransvea, T.E. O'Toole, L. Manzuk, B. Faha, and M. Hensler. 2002. Involvement of tumor cell integrin alpha v beta 3 in hematogenous metastasis of human melanoma cells. *Clin. Exp. Metastasis.* 19:427–436.
9. Rolli, M., E. Fransvea, J. Pilch, A. Saven, and B. Felding-Habermann. 2003. Activated integrin alphavbeta3 cooperates with metalloproteinase MMP-9 in regulating migration of metastatic breast cancer cells. *Proc. Natl. Acad. Sci. USA.* 100:9482–9487.
10. Gutheil, J.C., T.N. Campbell, P.R. Pierce, J.D. Watkins, W.D. Huse, D.J. Bodkin, and D.A. Cheresh. 2000. Targeted antiangiogenic therapy for cancer using Vitaxin: a humanized monoclonal antibody to the integrin alphavbeta3. *Clin. Cancer Res.* 6:3056–3061.
11. Brooks, P.C., R.A. Clark, and D.A. Cheresh. 1994. Requirement of vascular integrin alpha v beta 3 for angiogenesis. *Science.* 264: 569–571.
12. Brooks, P.C., A.M. Montgomery, M. Rosenfeld, R.A. Reisfeld, T. Hu, G. Klier, and D.A. Cheresh. 1994. Integrin alpha v beta 3 antagonists promote tumor regression by inducing apoptosis of angiogenic blood vessels. *Cell.* 79:1157–1164.
13. Dechantsreiter, M.A., E. Planker, B. Matha, E. Lohof, G. Holzemann, A. Jonczyk, S.L. Goodman, and H. Kessler. 1999. N-Methylated cyclic RGD peptides as highly active and selective alpha(V)beta(3) integrin antagonists. *J. Med. Chem.* 42:3033–3040.
14. Buerkle, M.A., S.A. Pahernik, A. Sutter, A. Jonczyk, K. Messmer, and M. Dellian. 2002. Inhibition of the alpha-V integrins with a cyclic RGD peptide impairs angiogenesis, growth and metastasis of solid tumours in vivo. *Br. J. Cancer.* 86:788–795.
15. Belvisi, L., T. Riccioni, M. Marcellini, L. Vesci, I. Chiarucci, D. Efrati, D. Potenza, C. Scolastico, L. Manzoni, K. Lombardo, et al. 2005. Biological and molecular properties of a new alpha(v)beta3/alpha(v)beta5 integrin antagonist. *Mol. Cancer Ther.* 4:1670–1680.
16. Reinmuth, N., W. Liu, S.A. Ahmad, F. Fan, O. Stoeltzing, A.A. Parikh, C.D. Bucana, G.E. Gallick, M.A. Nickols, W.F. Westlin, and L.M. Ellis. 2003. Alphavbeta3 integrin antagonist S247 decreases colon cancer metastasis and angiogenesis and improves survival in mice. *Cancer Res.* 63:2079–2087.
17. Beauvais, D.M., and A.C. Rapraeger. 2003. Syndecan-1-mediated cell spreading requires signaling by alpha(v)beta(3) integrins in human breast carcinoma cells. *Exp. Cell Res.* 286:219–232.
18. Beauvais, D.M., and A.C. Rapraeger. 2004. Syndecans in tumor cell adhesion and signaling. *Reprod. Biol. Endocrinol.* 2:3.
19. McQuade, K.J., D.M. Beauvais, B.J. Burbach, and A.C. Rapraeger. 2006. Syndecan-1 regulates alpha(v)beta(5) integrin activity in B82L fibroblasts. *J. Cell Sci.* 119:2445–2456.
20. Beauvais, D.M., B.J. Burbach, and A.C. Rapraeger. 2004. The syndecan-1 ectodomain regulates $\alpha_v\beta_3$ integrin activity in human mammary carcinoma cells. *J. Cell Biol.* 167:171–181.
21. Bernfield, M., M. Gotte, P.W. Park, O. Reizes, M.L. Fitzgerald, J. Lincecum, and M. Zako. 1999. Functions of cell surface heparan sulfate proteoglycans. *Annu. Rev. Biochem.* 68:729–777.
22. Alexopoulou, A.N., H.A. Multhaupt, and J.R. Couchman. 2007. Syndecans in wound healing, inflammation and vascular biology. *Int. J. Biochem. Cell Biol.* 39:505–528.
23. Woods, A. 2001. Syndecans: transmembrane modulators of adhesion and matrix assembly. *J. Clin. Invest.* 107:935–941.
24. McFall, A.J., and A.C. Rapraeger. 1998. Characterization of the high affinity cell-binding domain in the cell surface proteoglycan syndecan-4. *J. Biol. Chem.* 273:28270–28276.
25. McFall, A.J., and A.C. Rapraeger. 1997. Identification of an adhesion site within the syndecan-4 extracellular protein domain. *J. Biol. Chem.* 272:12901–12904.
26. Whiteford, J.R., and J.R. Couchman. 2006. A conserved NXIP motif is required for cell adhesion properties of the syndecan-4 ectodomain. *J. Biol. Chem.* 281:32156–32163.
27. Whiteford, J.R., V. Behrends, H. Kirby, M. Kusche-Gullberg, T. Muramatsu, and J.R. Couchman. 2007. Syndecans promote integrin-mediated adhesion of mesenchymal cells in two distinct pathways. *Exp. Cell Res.* 313:3902–3913.
28. Han, I., H. Park, and E.S. Oh. 2004. New insights into syndecan-2 expression and tumourigenic activity in colon carcinoma cells. *J. Mol. Histol.* 35:319–326.
29. Park, H., Y. Kim, Y. Lim, I. Han, and E.S. Oh. 2002. Syndecan-2 mediates adhesion and proliferation of colon carcinoma cells. *J. Biol. Chem.* 277:29730–29736.
30. Pampori, N., T. Hato, D.G. Stupack, S. Aidoudi, D.A. Cheresh, G.R. Nemerow, and S.J. Shattil. 1999. Mechanisms and consequences of affinity modulation of integrin alpha(v)beta(3) detected with a novel patch-engineered monovalent ligand. *J. Biol. Chem.* 274:21609–21616.
31. Tsukamoto, A.S., R. Grosschedl, R.C. Guzman, T. Parslow, and H.E. Varmus. 1988. Expression of the int-1 gene in transgenic mice is associated with mammary gland hyperplasia and adenocarcinomas in male and female mice. *Cell.* 55:619–625.
32. Imbert, A., R. Eelkema, S. Jordan, H. Feiner, and P. Cowin. 2001. ΔN89β-catenin induces precocious development, differentiation, and neoplasia in mammary gland. *J. Cell Biol.* 153:555–568.
33. Masson, V., L. Devy, C. Grignet-Debrus, S. Bernt, K. Bajou, S. Blacher, G. Roland, Y. Chang, T. Fong, P. Carmeliet, et al. 2002. Mouse aortic ring assay: a new approach of the molecular genetics of angiogenesis. *Biol. Proced. Online.* 4:24–31.
34. Kenyon, B.M., E.E. Voest, C.C. Chen, E. Flynn, J. Folkman, and R.J. D'Amato. 1996. A model of angiogenesis in the mouse cornea. *Invest. Ophthalmol. Vis. Sci.* 37:1625–1632.
35. Reinmuth, N., W. Liu, Y.D. Jung, S.A. Ahmad, R.M. Shaheen, F. Fan, C.D. Bucana, G. McMahon, G.E. Gallick, and L.M. Ellis. 2001. Induction of VEGF in perivascular cells defines a potential paracrine mechanism for endothelial cell survival. *FASEB J.* 15:1239–1241.
36. Gotte, M., A.M. Joussen, C. Klein, P. Andre, D.D. Wagner, M.T. Hinkes, B. Kirchhof, A.P. Adamis, and M. Bernfield. 2002. Role of syndecan-1 in leukocyte-endothelial interactions in the ocular vasculature. *Invest. Ophthalmol. Vis. Sci.* 43:1135–1141.
37. Lode, H.N., T. Moehler, R. Xiang, A. Jonczyk, S.D. Gillies, D.A. Cheresh, and R.A. Reisfeld. 1999. Synergy between an antiangiogenic integrin alphav antagonist and an antibody-cytokine fusion protein eradicates spontaneous tumor metastases. *Proc. Natl. Acad. Sci. USA.* 96:1591–1596.
38. Worapamorn, W., Y. Xiao, H. Li, W.G. Young, and P.M. Bartold. 2002. Differential expression and distribution of syndecan-1 and -2 in periodontal wound healing of the rat. *J. Periodontal Res.* 37:293–299.
39. Gallo, R., C. Kim, R. Kokenyesi, N.S. Adzick, and M. Bernfield. 1996. Syndecans-1 and -4 are induced during wound repair of neonatal but not fetal skin. *J. Invest. Dermatol.* 107:676–683.
40. Kainulainen, V., L. Nelimarkka, H. Jarvelainen, M. Laato, M. Jalkanen, and K. Elenius. 1996. Suppression of syndecan-1 expression in endothelial cells by tumor necrosis factor-alpha. *J. Biol. Chem.* 271:18759–18766.
41. Elenius, K., S. Vainio, M. Laato, M. Salmivirta, I. Thesleff, and M. Jalkanen. 1991. Induced expression of syndecan in healing wounds. *J. Cell Biol.* 114:585–595.
42. Li, J., L.F. Brown, R.J. Laham, R. Volk, and M. Simons. 1997. Macrophage-dependent regulation of syndecan gene expression. *Circ. Res.* 81:785–796.

43. Wang, H., S. Moore, and M.Z. Alavi. 1997. Expression of syndecan-1 in rabbit neointima following de-endothelialization by a balloon catheter. *Atherosclerosis*. 131:141–147.
44. Yuan, K., T.M. Hong, J.J. Chen, W.H. Tsai, and M.T. Lin. 2004. Syndecan-1 up-regulated by ephrinB2/EphB4 plays dual roles in inflammatory angiogenesis. *Blood*. 104:1025–1033.
45. Boudreau, N., C. Andrews, A. Srebrow, A. Ravanpay, and D.A. Cheresh. 1997. Induction of the angiogenic phenotype by Hox D3. *J. Cell Biol.* 139:257–264.
46. Boudreau, N.J., and J.A. Varner. 2004. The homeobox transcription factor Hox D3 promotes integrin alpha5beta1 expression and function during angiogenesis. *J. Biol. Chem*. 279:4862–4868.
47. Myers, C., A. Charboneau, and N. Boudreau. 2000. Homeobox B3 promotes capillary morphogenesis and angiogenesis. *J. Cell Biol.* 148:343–351.
48. Brown, E.J. 2002. Integrin-associated proteins. *Curr. Opin. Cell Biol.* 14:603–607.
49. McDonald, J.F., A. Zheleznyak, and W.A. Frazier. 2004. Cholesterol-independent interactions with CD47 enhance alpha(v)beta(3) avidity. *J. Biol. Chem*. 279:17301–17311.
50. Fujimoto, T.T., S. Katsutani, T. Shimomura, and K. Fujimura. 2003. Thrombospondin-bound integrin-associated protein (CD47) physically and functionally modifies integrin alpha(IIb)beta(3) by its extracellular domain. *J. Biol. Chem*. 278:26655–26665.
51. Boettiger, D., F. Huber, L. Lynch, and S. Blystone. 2001. Activation of alpha(v)beta(3)-vitronectin binding is a multistage process in which increases in bond strength are dependent on Y747 and Y759 in the cytoplasmic domain of beta(3). *Mol. Biol. Cell.* 12:1227–1237.
52. Yan, B., D.D. Hu, S.K. Knowles, and J.W. Smith. 2000. Probing chemical and conformational differences in the resting and active conformers of platelet integrin alpha(IIb)beta(3). *J. Biol. Chem*. 275:7249–7260.
53. Du, X.P., E.F. Plow, A.L. Frelinger III, T.E. O'Toole, J.C. Loftus, and M.H. Ginsberg. 1991. Ligands "activate" integrin alpha(IIb)beta(3) (platelet GPIIb-IIIa). *Cell*. 65:409–416.
54. Frelinger, A.L., III, X.P. Du, E.F. Plow, and M.H. Ginsberg. 1991. Monoclonal antibodies to ligand-occupied conformers of integrin alpha(IIb)beta(3) (glycoprotein IIb-IIIa) alter receptor affinity, specificity, and function. *J. Biol. Chem*. 266:17106–17111.
55. Humphries, M.J. 1996. Integrin activation: the link between ligand binding and signal transduction. *Curr. Opin. Cell Biol.* 8:632–640.
56. Takagi, J., B.M. Petre, T. Walz, and T.A. Springer. 2002. Global conformational rearrangements in integrin extracellular domains in outside-in and inside-out signaling. *Cell*. 110:599–611.
57. Tadokoro, S., S.J. Shattil, K. Eto, V. Tai, R.C. Liddington, J.M. de Pereda, M.H. Ginsberg, and D.A. Calderwood. 2003. Talin binding to integrin beta tails: a final common step in integrin activation. *Science*. 302:103–106.
58. Wegener, K.L., A.W. Partridge, J. Han, A.R. Pickford, R.C. Liddington, M.H. Ginsberg, and I.D. Campbell. 2007. Structural basis of integrin activation by talin. *Cell*. 128:171–182.
59. Li, R., N. Mitra, H. Gratkowski, G. Vilaire, R. Litvinov, C. Nagasami, J.W. Weisel, J.D. Lear, W.F. DeGrado, and J.S. Bennett. 2003. Activation of integrin alpha(IIb)beta(3) by modulation of transmembrane helix associations. *Science*. 300:795–798.
60. Jalkanen, M., H. Nguyen, A. Rapraeger, N. Kurn, and M. Bernfield. 1985. Heparan sulfate proteoglycans from mouse mammary epithelial cells: localization on the cell surface with a monoclonal antibody. *J. Cell Biol.* 101:976–984.
61. David, G., B. van der Schueren, P. Marynen, J.J. Cassiman, and H. van den Berghe. 1992. Molecular cloning of amphiglycan, a novel integral membrane heparan sulfate proteoglycan expressed by epithelial and fibroblastic cells. *J. Cell Biol.* 118:961–969.
62. Alexander, C.M., F. Reichsman, M.T. Hinkes, J. Lincecum, K.A. Becker, S. Cumberledge, and M. Bernfield. 2000. Syndecan-1 is required for Wnt-1-induced mammary tumorigenesis in mice. *Nat. Genet*. 25:329–332.
63. Liu, B.Y., Y.C. Kim, V. Leatherberry, P. Cowin, and C.M. Alexander. 2003. Mammary gland development requires syndecan-1 to create a beta-catenin/TCF-responsive mammary epithelial subpopulation. *Oncogene*. 22:9243–9253.
64. Chandrakasan, G., D.A. Torchia, and K.A. Piez. 1976. Preparation of intact monomeric collagen from rat tail tendon and skin and the structure of the nonhelical ends in solution. *J. Biol. Chem*. 251:6062–6067.
65. Yatohgo, T., M. Izumi, H. Kashiwagi, and M. Hayashi. 1988. Novel purification of vitronectin from human plasma by heparin affinity chromatography. *Cell Struct. Funct*. 13:281–292.
66. Gumkowski, F., G. Kaminska, M. Kaminski, L.W. Morrissey, and R. Auerbach. 1987. Heterogeneity of mouse vascular endothelium. In vitro studies of lymphatic, large blood vessel and microvascular endothelial cells. *Blood Vessels*. 24:11–23.
67. Ades, E.W., F.J. Candal, R.A. Swerlick, V.G. George, S. Summers, D.C. Bosse, and T.J. Lawley. 1992. HMEC-1: establishment of an immortalized human microvascular endothelial cell line. *J. Invest. Dermatol.* 99:683–690.
68. Laemmli, U.K. 1970. Cleavage of structural proteins during the assembly of the head of bacteriophage T4. *Nature*. 227:680–685.